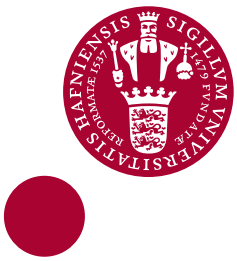

Syndecan-4 Protects the Heart From the Profibrotic Effects of Thrombin-Cleaved Osteopontin

Herum, Kate M; Romaine, Andreas; Wang, Ariel; Melleby, Arne Olav; Strand, Mari E; Pacheco, Julian; Braathen, Bjørn; Dunér, Pontus; Tønnessen, Theis; Lunde, Ida G; Sjaastad, Ivar; Brakebusch, Cord; McCulloch, Andrew D; Gomez, Maria F; Carlson, Cathrine R; Christensen, Geir

Published in:
Journal of the American Heart Association

DOI:
10.1161/JAHA.119.013518

Publication date:
2020

Document version
Publisher's PDF, also known as Version of record

ORIGINAL RESEARCH

Syndecan-4 Protects the Heart From the Profibrotic Effects of Thrombin-Cleaved Osteopontin

Kate M. Herum, PhD; Andreas Romaine, MS; Ariel Wang, BS; Arne Olav Melleby, MS; Mari E. Strand, PhD; Julian Pacheco, BS; Bjørn Braathen, MD, PhD; Pontus Dunér, PhD; Theis Tønnessen, MD, PhD; Ida G. Lunde, PhD; Ivar Sjaastad, MD, PhD; Cord Brakebusch, PhD; Andrew D. McCulloch, PhD; Maria F. Gomez, PhD; Cathrine R. Carlson, PhD; Geir Christensen, MD, PhD

***Background*—**Pressure overload of the heart occurs in patients with hypertension or valvular stenosis and induces cardiac fibrosis because of excessive production of extracellular matrix by activated cardiac fibroblasts. This initially provides essential mechanical support to the heart, but eventually compromises function. Osteopontin is associated with fibrosis; however, the underlying signaling mechanisms are not well understood. Herein, we examine the effect of thrombin-cleaved osteopontin on fibrosis in the heart and explore the role of syndecan-4 in regulating cleavage of osteopontin.

***Methods and Results*—**Osteopontin was upregulated and cleaved by thrombin in the pressure-overloaded heart of mice subjected to aortic banding. Cleaved osteopontin was higher in plasma from patients with aortic stenosis receiving crystalloid compared with blood cardioplegia, likely because of less heparin-induced inhibition of thrombin. Cleaved osteopontin and the specific osteopontin peptide sequence RGDSLAYGLR that is exposed after thrombin cleavage both induced collagen production in cardiac fibroblasts. Like osteopontin, the heparan sulfate proteoglycan syndecan-4 was upregulated after aortic banding. Consistent with a heparan sulfate binding domain in the osteopontin cleavage site, syndecan-4 was found to bind to osteopontin in left ventricles and cardiac fibroblasts and protected osteopontin from cleavage by thrombin. Shedding of the extracellular part of syndecan-4 was more prominent at later remodeling phases, at which time levels of cleaved osteopontin were increased.

***Conclusions*—**Thrombin-cleaved osteopontin induces collagen production by cardiac fibroblasts. Syndecan-4 protects osteopontin from cleavage by thrombin, but this protection is lost when syndecan-4 is shed in later phases of remodeling, contributing to progression of cardiac fibrosis. **(*J Am Heart Assoc*. 2020;9:e013518. DOI: 10.1161/JAHA.119.013518.)**

Key Words: aortic stenosis • cardiac fibroblasts • left ventricular fibrosis • extracellular matrix • mechanical • myofibroblast • pressure overload • stiffness

In response to injury and pressure overload, cardiac fibroblasts start to proliferate and produce excessive amounts of extracellular matrix (ECM) proteins.[1] Activation also leads to the differentiation of fibroblasts into more contractile myofibroblasts, providing initially an essential mechanical support to withstand the increased pressure in the left ventricle. However, myofibroblast activity and excessive ECM production, if persistent, can lead to cardiac fibrosis, increased stiffness and, hence, impaired diastolic function.[2] Although there are currently ongoing clinical trials aiming at preventing or reducing cardiac fibrosis, there is yet no effective medical treatment available. A better understanding of the molecular basis of fibroblast activation and fibrosis is necessary to identify novel targets for the treatment of cardiac fibrosis and heart failure.[3]

From the Institute for Experimental Medical Research, Oslo University Hospital and University of Oslo, Norway (K.M.H., A.R., A.O.M., M.E.S., T.T., I.G.L., I.S., C.R.C., G.C.); KG Jebsen Center for Cardiac Research, University of Oslo, Norway (K.M.H., A.R., A.O.M., M.E.S., I.G.L., I.S., C.R.C., G.C.); Center for Heart Failure Research (K.M.H., A.R., A.O.M., M.E.S., I.G.L., I.S., C.R.C., G.C.) and Department of Cardiothoracic Surgery (B.B., T.T.), Oslo University Hospital, Oslo, Norway; Departments of Bioengineering (K.M.H., A.W., J.P., A.D.M.) and Medicine (A.D.M.), University of California, San Diego, La Jolla, CA (K.M.H., A.W., J.P., A.D.M.); Biotech Research & Innovation Centre, University of Copenhagen, Denmark (K.M.H., C.B.); Department of Clinical Sciences, Lund University Diabetes Centre, Lund University, Malmö, Sweden (P.D., M.F.G.).

Accompanying Tables S1, S2 and Figures S1 through S10 are available at https://www.ahajournals.org/doi/suppl/10.1161/JAHA.119.013518

Correspondence to: Maria F. Gomez, PhD, Department of Clinical Sciences, Lund University, Jan Waldenströms gata 35, CRC 91:12, S-214 28 Malmö, Sweden. E-mail: maria.gomez@med.lu.se

Received September 10, 2019; accepted November 5, 2019.

Clinical Perspective

What Is New?

- Extracellular cleaved osteopontin promotes collagen expression by cardiac fibroblasts.
- The heparan sulfate proteoglycan syndecan-4 binds and protects osteopontin from cleavage in the heart during the early phases of remodeling.
- This protection is lost when syndecan-4 ectodomain is shed in later phases of remodeling.

What Are the Clinical Implications?

- Preventing osteopontin cleavage or inhibiting profibrotic effects of cleaved osteopontin could potentially be used to treat cardiac fibrosis.

Proteoglycans are emerging as important regulators of fibroblast activation and fibrosis in the heart.[4,5] We have previously shown that the transmembrane proteoglycan syndecan-4 induces myofibroblast differentiation and expression of ECM proteins, such as collagen, in mechanically stressed cardiac fibroblasts via activation of the calcineurin/nuclear factor of activated T cells signaling pathway.[6] Accordingly, upregulation of collagen I and III, the most dominant collagens in the heart, was blunted in the left ventricle of mice lacking syndecan-4 during the early phase of remodeling (24 hours) in the pressure overloaded heart. However, this difference in collagen levels was no longer observed in the later phase of remodeling (after 7 days),[7] indicating that after the initial phase cardiac fibroblasts from syndecan-4 knockout mice exhibited a higher collagen accumulation rate than fibroblasts from wild-type (WT) mice. Thus, our published data indicate a dual role for syndecan-4 in collagen regulation: promoting collagen expression in the early phase of cardiac remodeling through calcineurin/nuclear factor of activated T cell signaling[6] and limiting collagen expression in the late phase via an unknown mechanism.

The extracellular domain of syndecan-4 is substituted with heparan sulfate glycosaminoglycan chains that have been shown to bind and regulate various cytokines and growth factors.[8–11] One of these is osteopontin, a matricellular protein that has recently emerged not only as a marker of cardiac fibrosis and heart failure but as an active regulator of these processes.[7,12–22] Plasma osteopontin has been suggested as a predictive biomarker of cardiovascular death and urgent heart failure hospitalization in patients with dilated cardiomyopathy.[22] In mouse primary cardiac fibroblasts plated on fibronectin-coated plates, we have previously found that myofibroblast differentiation induces osteopontin expression.[7] The mechanisms by which osteopontin induces fibrosis in the heart remain unclear, but recent data suggest that cleavage of osteopontin by thrombin promotes its fibrogenic effects.[23] Indeed, thrombin was recently found to be upregulated in patients with heart failure,[15] and inhibition of thrombin reduced fibrosis and improved diastolic function in mice with left ventricular pressure overload.[24]

Interestingly, the thrombin cleavage site is located within a heparan sulfate binding motif in osteopontin, which in liver has been found to bind to the heparan sulfate glycosaminoglycan chains of syndecan-4, protecting osteopontin from being cleaved by thrombin.[10] Whether this is true in the heart is not known. Herein, we examine the levels of expression and degree of cleavage of osteopontin in the mouse heart in the early (<3 days) and late (≥3 days) phases of remodeling after aortic banding (AB) and the effects of full-length osteopontin (FL-OPN) versus thrombin-cleaved osteopontin (cl-OPN) on cardiac fibroblast profibrotic activity. Furthermore, we examine whether syndecan-4 binds and protects osteopontin from cleavage by thrombin in the pressure-overloaded heart and the potential role of syndecan-4 shedding on osteopontin cleavage in the late phase of remodeling.

Methods

The data that support the findings of this study are available from the corresponding author on reasonable request.

Blood Samples From Patients With Aortic Stenosis

The study protocol for human blood sampling and myocardial biopsies was reviewed and approved by the Regional Committee for Medical Research Ethics (approval Nos. REK 290-06114 and REK 2018/1870, respectively) and conformed to the Declaration of Helsinki. Informed written consent was obtained from all patients. Blood samples from 30 patients undergoing aortic valve replacement caused by severe, symptomatic aortic stenosis at Oslo University Hospital Ullevål (Oslo, Norway) were included in this study. Patients received either cold blood cardioplegia or cold crystalloid cardioplegia, as previously described.[25] Samples were drawn during open heart surgery from a coronary sinus catheter and from the cannulated radial artery immediately after onset of cardiopulmonary bypass. Levels of cl-OPN/FL-OPN were measured in plasma using ELISA (human anti-osteopontin JP27158 and human anti–N-osteopontin JP27258; IBL, Hamburg, Germany), according to the manufacturer's instructions. Analyses were performed with and without 2 statistical outliers, determined by Tukey's fences derived from the interquartile range. Myocardial biopsies were obtained from

the left ventricular free wall near the apex of the heart, during aortic valve replacement surgery. Control samples were obtained from normal myocardium from the same area, of patients undergoing surgery for coronary artery disease.

Animals and Pressure Overload Model

AB or sham operation was performed on 8- to 12-week-old male WT C57BL/6JBomTac (Taconic, Denmark) and syndecan-4 knockout (Sdc4$^{-/-}$) mice,[26] as previously described.[27] Successful AB was determined by echocardiography 24 hours after AB, using the inclusion criteria of aortic flow velocity >4 m/s for successful AB. Echocardiographic assessment of left ventricular and atria dimensions in diastole and systole was performed by I.S. blinded to group, in lightly anesthetized mice breathing 1.5% isoflurane through a mask, using VEVO 2100 (VisualSonics, Toronto, ON, Canada). Mice were euthanized by cervical dislocation after 24 hours, 3 days, 7 days, or 21 days after AB; and cardiac tissue was harvested for further analysis. Blood samples were collected from the abdominal aorta 3 days after banding before termination of the experiment and used for plasma osteopontin measurements using ELISA (mouse anti-osteopontin JP27351; IBL), according to the manufacturer's instructions. For isolation of neonatal or adult cardiac fibroblasts, WT C57Bl/6J (000664; The Jackson Laboratory, Bar Harbor, ME) or collagen1a1–GFP (green fluorescent protein) reporter mice (provided by David Brenner, University of California San Diego, La Jolla, CA, USA and characterized by researchers[28–30]) were used. Animals were handled according to the National Regulation on Animal Experimentation in accordance with the Norwegian Animal Welfare Act and the *Guide for the Care and Use of Laboratory Animals* (eighth edition). The protocols were approved by the Norwegian National Animal Research Committee (protocol No. 2845) and the University of California, San Diego, Animal Subjects Committee (protocol No. S01013M).

Left Ventricular Lysate for Immunoblotting

Frozen left ventricular tissue from mice was homogenized with a Polytron PT 1200 CL in a homogenization buffer containing 1% Triton and 0.1% Tween 20 in PBS with protease (Complete EDTA-free tablets; Roche Diagnostics) and phosphatase inhibitors (PhosSTOP; Roche; 04906837001). After 30 minutes on ice, the samples were centrifuged at 21 000*g* for 10 minutes at 4°C. The supernatant was collected and stored at −70°C before further analysis. Some samples were treated with heparan sulphate–degrading enzymes heparitinase I, heparitinase II, heparitinase III, and chondritinase cABC (all from AMSBIO), as described,[31] to cut off glycosaminoglycan chains from syndecan-4.

Native Gels, Immunoblotting, and Osteopontin Blocking Experiment

The following antibodies were used as primary antibodies for immunoblotting: anti-osteopontin (1:500 dilution; IBL), anti-osteopontin (1:1000 dilution; ab181440; Abcam, Cambridge, UK), anti-osteopontin (1:400 dilution; sc-20788; Santa Cruz Biotechnology), anti–syndecan-4 targeting intracellular domain (1:1000 dilution; custom made from Genscript Corp[27]), anti–syndecan-4 targeting extracellular domain (sc-15350; Santa Cruz Biotechnology; or a custom-made antibody from Genscript; 1:1000 dilution), anti–collagen I (1:500 dilution; NBP1-30054; Novus Biological, Centennial, CO), anti-GAPDH (1:500; sc-20357; Santa Cruz Biotechnology), anti-vinculin (1:960 000 dilution; V9131; Sigma Aldrich), and anti-fibronectin extra domain A (1:400 dilution; F6140; Sigma). Horseradish peroxidase–conjugated anti-rabbit IgG (osteopontin and syndecan-4) and anti-mouse IgG (vinculin) (1:5000 dilution; catalog Nos. NA934V and NA931V, respectively; GE Healthcare, Oslo, Norway) were used as secondary antibodies. Protein (90 μg) in a native sample buffer (No. 161-0738; BioRad Laboratories, Munich, Germany) was analyzed on 4% to 15% Criterion Tris-HCL gels (No. 345-0028; BioRad Laboratories) without 0.1% SDS and in running buffer (25 mmol/L Tris and 192 mmol/L glycine, pH 8.3; No. 161-0771; BioRad Laboratories) at 130 V for 120 minutes. For reducing conditions, the lysates and immunoprecipitations were boiled in an SDS-containing loading buffer and analyzed on 15% Criterion Tris-HCl gels (No. 345-0020) in an SDS-containing running buffer (25 mmol/L Tris, 192 mmol/L glycine, and 0.1% SDS, pH 8.3; No. 161-0772; BioRad Laboratories). Proteins were blotted onto polyvinylidene difluoride membranes (RPN 303F; GE Healthcare) at 100 V for 50 minutes. The polyvinylidene difluoride membranes were blocked in 3% BSA (Rinderalbumin; catalog No. 805095; BioRad) or 1% casein (Western blocking reagent; catalog No. 11921681001; Roche) in Tris-buffered saline/Tween 20 for 60 minutes at room temperature, incubated with primary antibodies overnight at 4°C, washed 3 times at 5 minutes in Tris-buffered saline/Tween 20, and incubated with a horseradish peroxidase–conjugated secondary antibody. Blots were developed by using ECL Plus (RPN2132; GE Healthcare), and chemiluminescence signals were detected by Las-4000 (Fujifilm, Tokyo, Japan). The membranes were stripped with restore Western blot stripping buffer (No. 21059; Thermo Scientific, Rockford, IL) for 30 minutes at room temperature and washed 3 times for 10 minutes in Tris-buffered saline/Tween 20 between each antibody. For the osteopontin blocking experiment, anti-osteopontin (1:1000 dilution; ab181440) was preincubated with or without 5 μmol/L of the osteopontin blocking peptide (Genscript Corp) overnight at 4°C before immunoblotting for 2 hours at room temperature.

Immunoprecipitation

Lysates from NIH 3T3 fibroblast cells (CRL-1658; ATCC, Manassas, VA) or rat neonatal cardiac fibroblasts were incubated in presence of 2 mmol/L $CaCl_2$ with anti–syndecan-4 (No. 550350; BD) or normal rat IgG (sc-2027; Santa Cruz Biotechnology; negative control) precoupled onto magnetic beads (Dynabeads antibody coupling kit; No. 14311D) overnight at 4°C. Immunocomplexes were washed 3 times in immunoprecipitation buffer (20 mmol/L HEPES, pH 7.5, 150 mmol/L NaCl, 1 mmol/L EDTA, and 1.5% Triton) boiled in SDS loading buffer and analyzed by immunoblotting. Recombinant mouse syndecan-4 (Fc-tag at C-terminus; No. 50726-M02H; Sino Biological Inc) and recombinant human osteopontin (No. 120-35; Peprotech) proteins were used as positive controls for immunoblotting.

Peptide Array Synthesis, Epitope Mapping, and Osteopontin Blocking Peptide

Mouse, rat, and human osteopontin protein sequences were synthesized as 20-mer peptides with a 3–amino acid shift on cellulose membranes using a Multipep automated peptide synthesizer (INTAVIS Bioanalytical Instruments AG, Cologne, Germany), as described previously.[32] The osteopontin blocking peptide covering the ab181440 antigen epitope LLAPQNAVSSEEKDDFKQETLPSNSNESHDHM (amino acids 53–84 in mouse osteopontin) was synthesized with a purity of 94.5% by Genscript Corp.

Gene Expression Analysis

RNA was extracted from frozen left ventricles and cell cultures using the RNeasy Mini Kit (Qiagen, Hilden, Germany). cDNA synthesis was performed using the iScript cDNA Synthesis Kit (BIO-RAD, Hercules, CA). Quantitative real-time polymerase chain reaction was used to assess gene expression using predesigned validated TaqMan assays (Applied Biosystems, Foster City, CA) for osteopontin (*Spp1*; Mm00436767_m1), syndecan-4 (*Sdc4*; Mm00488527_m1), collagen I (*Col1a2*; Mm00483888_m1), collagen III (*Col3a1*; Mm00802331_m1), transforming growth factor β1 (*Tgfb1*; Mm00441726_m1), decorin (*Dcn*; Mm00514535_m1), smooth muscle α-actin (SMA; *Acta2*; Mm01546133_m1), SM22 (*transgelin*; Mm00441660_m1), thrombin (*coagulation factor II*; Mm00438843_m1), matrix metalloproteinase (MMP) 2 (Mm00439506_m1), MMP3 (Mm00440295_m1), MMP7 (Mm00487724_m1), MMP9 (Mm00442991_m1), Rpl32 (Hs00851655_g1), and GAPDH (*Gapdh*; Mm03302249_g1) or KAPA SYBR Fast Universal qPCR kit (catalog No. 07959397001; Kapa Biosystems, Cape Town, South Africa) and primers targeting *Col1a1* (5′-GCTCCTCTTAGGGGCCACT-3′ and 5′-CCACGTCTCACCATTGGGG-3′), *Tgfb1* (5′-CTCCCGTGGCTTCTAGTGC-3′ and 5′-GCCTTAGTTTGGACAGGATCTG-3′), and *Gapdh* (5′-AGGTCGGTGTGAACGGATTTG-3′ and 5′-TGTAGACCATGTAGTTGAGGTCA-3′) from Integrated DNA Technologies (Indianapolis, IN). Data were normalized to GAPDH.

Immunohistochemistry

Tissues were fixed in 10% buffered formalin, embedded in paraffin, divided into sections (4-μm thickness), and stained with an antibody against FL-OPN (R1565; Acris) and an antibody specifically targeting the N-terminal fragment of cl-OPN (anti–N-osteopontin; JP11108; IBL; epitope mapped in Figure S1A). FL-OPN and cl-OPN were quantified using stained midventricular heart sections from WT mice that had been sham or AB operated. Blinded image analyses were performed using Zen 2 (blue edition; Zeiss). Briefly, sections were digitized using a ×20 objective and thresholding of osteopontin staining was set and kept consistent for all images. Pixel areas negative or positive for osteopontin staining were calculated, and osteopontin staining was represented as percentage positive pixels of total pixels. Primary antibodies were omitted to control for unspecific binding of the secondary antibodies (Figure S2). Images were acquired using Zeiss AxioScan Z1 slide scanner or Axioskop 2.

Fibroblast Cell Cultures, Cyclic Stretch, and Stimulation With Osteopontin Variants

Neonatal or adult cardiac fibroblasts from WT C57Bl/6J (000664; The Jackson Laboratory, Bar Harbor, ME) or col1a1-GFP reporter mice (provided by David Brenner and characterized by researchers[28–30]) were isolated, as previously described,[33] and used at passage 2 to limit in vitro effects on fibroblast phenotype or plated directly on polyacrylamide hydrogels fabricated as previously described.[33] Elastic moduli *E* of polyacrylamide gels were set to 4.5 or 40 kPa by adjusting the relative acrylamide and bis-acrylamide concentrations.[34] Gels were coated with collagen type 1. Cardiac fibroblasts were plated on fibronectin-coated coverslips to induce myofibroblast differentiation.[6] Human fibrosarcoma HT1080 were purchased from ATCC (CCL-121). Cells were cultured in DMEM (41965; GIBCO-BRL, Invitrogen, Paisley, UK) supplemented with 10% FCS (14-701E; Bio-Whittaker, Lonza, Basel, Switzerland) and penicillin/streptomycin (G6784; Sigma, St Louis, MO). Cyclic stretch (10%; 1 Hz; 24 hours) was applied using the FlexCell Tension System FX-4000 (Dunn Labortechnik, Asbach, Germany). Cells were stimulated with 250 ng/mL recombinant mouse osteopontin (441-OP; R&D systems), cl-OPN, a synthetic peptide (RGDSLAYGLR) of the cryptic osteopontin sequence revealed on cleavage of osteopontin by thrombin, heat-treated thrombin (37°C for 16 hours), TGFβ1 (2.5 ng/mL; 14-8342-

62; ThermoFisher Scientific), and the TGFβ receptor (TGFβR) I inhibitor SB431542 (5 μmol/L; 1614; Tocris).

In Vitro Cleavage of Recombinant Osteopontin

Recombinant osteopontin (5 μg) was cleaved by incubation with 0.002 U/μL recombinant thrombin (1473-SE; R&D Systems) at 37°C for 16 hours and used for cardiac fibroblast stimulations. To investigate whether syndecan-4 could protect osteopontin from cleavage by thrombin, recombinant extracellular domain of syndecan-4 (Sino Biological Inc, Beijing, China) and osteopontin were preincubated for 1 hour at 37°C in a 1:2 ratio before 30 minutes of incubation with thrombin. For stimulation of cardiac fibroblasts, FL-OPN was also incubated at 37°C for 16 hours. Although inactive after incubation, thrombin is also present in the product that we use for stimulating cells. To control for unspecific effect of inactive thrombin, a control containing only thrombin was included in all experiments.

Immunocytochemistry

Cells grown on fibronectin-coated glass coverslips were fixed in 4% paraformaldehyde and stained using anti-SMA (Sigma, Schnelldorf, Germany), anti-osteopontin (sc-20788), anti–syndecan-4 (BD; No. 550350), and Alexa Fluor secondary antibodies (Invitrogen, Paisley, UK). Cells grown on fibronectin-coated glass coverslips were fixed in 4% paraformaldehyde (Sigma) and stained using mouse anti-SMA (1:300; Sigma) and Alexa Fluor 488–secondary anti-mouse antibodies (Invitrogen). Images were obtained using an LSM 710 confocal microscope (Zeiss). Nuclei were stained with Sytox orange (Invitrogen), and omitting primary antibodies served as negative controls.

Statistical Analysis

Data are expressed as mean±SEM. Normality was tested using the D'Agostino and Pearson omnibus normality test, and parametric or nonparametric testing was performed, depending on the outcomes. Repeated-measures ANOVA or 1- or 2-way ANOVA, followed by Tukey's or Holm-Sidak's multiple comparisons test, Wilcoxon matched-pairs signed rank test, Mann-Whitney test, and Student *t* tests, was used.

Results

cl-OPN Is Increased in the Pressure-Overloaded Heart

Osteopontin mRNA was increased 24 hours, 3 days, 7 days, and 21 days after inducing pressure overload by AB, with a massive 700-fold increase in mRNA expression at 24 hours (Figure 1A). This resulted in increased plasma levels of FL-OPN measured 3 days after AB (Figure 1B), at which time left ventricular weight was increased (Figure 1C). We have previously demonstrated that plating cardiac fibroblasts on fibronectin-coated plates, a procedure known to trigger myofibroblast differentiation, results in increased osteopontin mRNA.[7] Herein, we show that osteopontin mRNA increases in response to cyclic stretch (Figure 1D), showing that osteopontin gene regulation is mechanosensitive in cardiac fibroblasts.

We next examined the presence of FL-OPN and cl-OPN in the pressure-overloaded heart in mice subjected to AB. Mouse left ventricular tissue sections showed a substantial increase in both FL-OPN and cl-OPN staining 3 days after AB (Figure 1E and 1F), with cl-OPN expressed in the vicinity of blood vessels and in the interstitial space (Figure 1E). Using validated primers, thrombin mRNA was not detected in mouse left ventricular tissue lysates by quantitative polymerase chain reaction, suggesting that the source of thrombin is likely from the circulation.

To gain insight on osteopontin expression and cleavage in the human pressure-overloaded heart, we measured cl-OPN and FL-OPN in plasma, and osteopontin mRNA in myocardial biopsies, from patients with aortic stenosis undergoing aortic valve replacement surgery. Patients (Table S1) receiving cold crystalloid cardioplegia to induce cardiac arrest during surgery had more cl-OPN/FL-OPN in plasma compared with patients receiving cold blood cardioplegia (Figure 1G). This may be caused by the more diluted heparin levels likely faced by the heart during the cardiac arrest period in the crystalloid cardioplegia group and, hence, concomitantly reduced inhibition of thrombin. Furthermore, cl-OPN/FL-OPN showed a trend (P=0.07; N=28; Wilcoxon matched-pairs signed rank test) to be higher in plasma from the coronary sinus versus plasma from the radial artery, indicating that osteopontin might be cleaved locally in the pressure-overloaded human heart. Analyses of data with outliers are shown in Figure S3. Osteopontin mRNA was not increased in myocardial biopsies from patients with aortic stenosis (Figure 1H).

cl-OPN, But Not FL-OPN, Increases Collagen I Expression in Cardiac Fibroblasts

To examine the effect of cl-OPN on cardiac fibroblast function and phenotype in vitro, recombinant FL-OPN was cleaved by incubation with thrombin. Cleavage was confirmed by Western blot, showing a shift of the 60-kDa FL-OPN to the smaller 40-kDa cl-OPN band consisting of the N-terminal thrombin-cleaved fragment of osteopontin (Figure 2A). Because the solution of cl-OPN also contained thrombin, which alone has been shown to induce fibrotic activity,[35] a

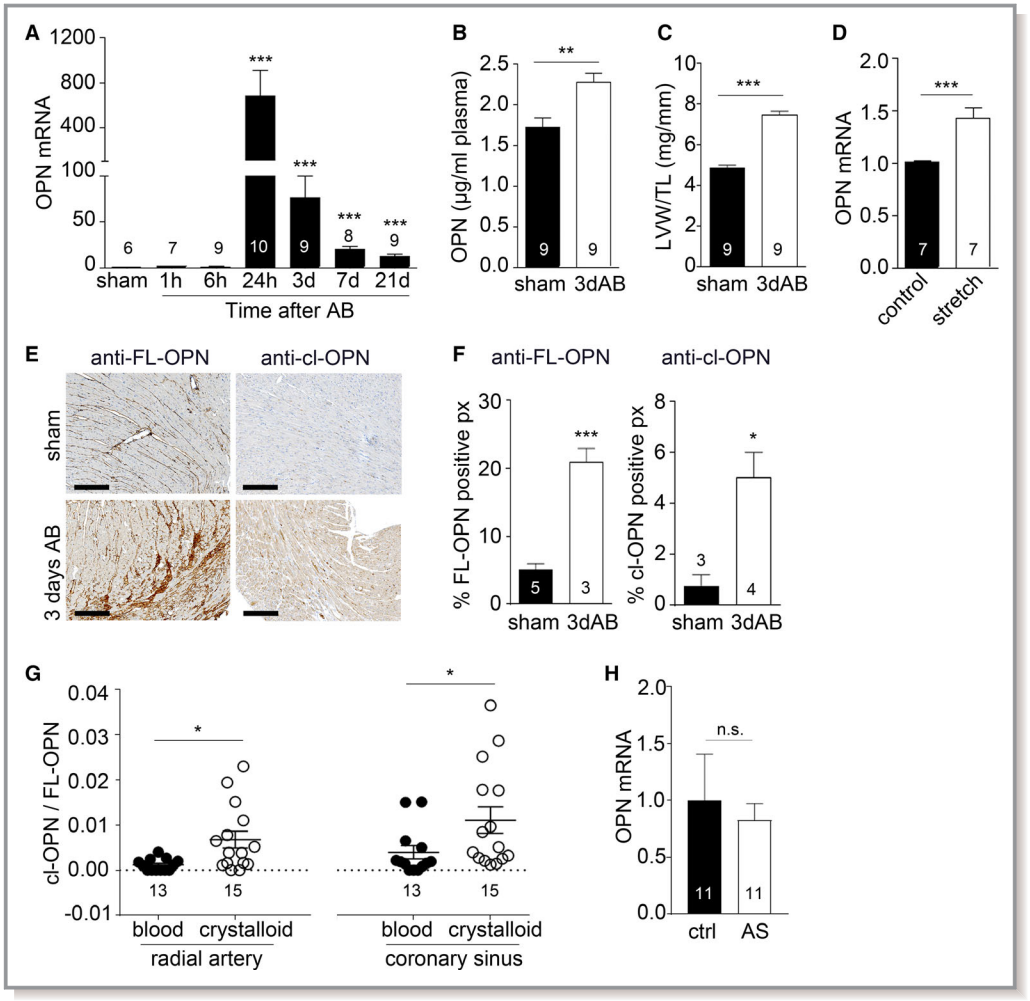

Figure 1. Cardiac expression and cleavage of osteopontin is induced by left ventricular pressure overload. **A**, Osteopontin mRNA levels in left ventricular tissue after aortic banding (AB) relative to sham-operated animals for each time point. The 24-hour and 7-day time points were previously published.[7] **B**, Osteopontin protein in mouse plasma 3 days after AB. **C**, Left ventricular weight (LVW) relative to tibia length (TL) in sham and 3-day AB mice. **D**, Osteopontin mRNA levels after stretching cardiac fibroblasts in vitro. **E**, Micrographs of full-length osteopontin (FL-OPN) and N-terminal fragment of thrombin-cleaved osteopontin (cl-OPN) detected by immunohistochemistry of left ventricular tissue sections from mice 3 days after AB or sham operation (bar=200 µm). **F**, Quantification of osteopontin-positive pixels relative to total number of pixels analyzed of micrographs, as represented in **E**. **G**, cl-OPN protein levels relative to FL-OPN in plasma from the coronary sinus and radial artery of patients with aortic stenosis (AS) receiving blood cardioplegia or crystalloid cardioplegia. **H**, Osteopontin mRNA normalized to Rpl32 in myocardial biopsies from patients with AS and controls. Student unpaired *t* test was used to determine significant changes. Numbers are indicated in graphs. **P*<0.05, ***P*<0.01, ****P*<0.005.

control containing thrombin only was used to account for effects independent of cl-OPN.

Although stimulation with FL-OPN for 24 hours had no effect on the mRNA expression of collagen 1a1, collagen 3a1, or TGFβ, stimulation with cl-OPN increased the expression of collagen 1a2 and collagen 3a1 (Figure 2B). Stimulation with cl-OPN also translated into increased collagen I protein (Figure 2C).

We also investigated if the profibrotic activity of cl-OPN could be driven by the specific sequence RGDSLAYGLR that is exposed after thrombin cleavage (underlined in Figure S1A). To test the effects of the RGDSLAYGLR peptide under more controlled physiological culturing conditions, we cultured cardiac fibroblasts on soft and stiff polyacrylamide hydrogels. These gels generate 4.5 and 40 kPa stiffness, which resemble the stiffness of the healthy and fibrotic myocardium, respectively.[33,36–38] In cardiac fibroblasts cultured on 40-kPa gels, stimulation with the RGDSLAYGLR peptide increased collagen 1a1 mRNA, but no effect was observed when cells were cultured on 4.5-kPa gels (Figure 2D). In contrast, TGFβ

stimulation increased collagen 1a1 mRNA only when cells were cultured on 4.5-kPa gels (Figure 2E). Interestingly, TGFβ mRNA measured in left ventricular tissue lysates peaked 24 hours after AB, after which expression gradually decreased (Figure S4A). This reduction was accompanied by increased expression of its natural inhibitor decorin[39] (Figure S4B), suggesting that availability of TGFβ may decrease with time after AB.

To study the interaction between the RGDSLAYGLR peptide and TGFβ signaling, we used adult cardiac fibroblasts from COL1A1-GFP reporter mice that expressed GFP under the control of the COL1A1 promoter.[28–30] No synergistic effect was observed when cells were costimulated with the peptide and TGFβ (Figure 2F and 2G), suggesting they both may be engaging the same signaling pathways to alter collagen 1a1 expression. Indeed, stimulation of cardiac fibroblasts with TGFβ or the RGDSLAYGLR peptide in the presence of the TGFβRI blocker SB431542 no longer impacted collagen 1a1 expression (Figure 2F and 2G). SB431542 was also able to block the stimulatory effect of the RGDSLAYGLR peptide on collagen 1a1 mRNA that was observed in cardiac fibroblasts cultured on 40-kPa gels (Figure 2H). Stimulation with the RGDSLAYGLR peptide did not alter TGFβ mRNA expression (Figure 2I).

We previously demonstrated transiently increased expression of the cell cycle S-phase marker, proliferating cell nuclear antigen (PCNA), in cardiac homogenates after AB and that this PCNA signal could be attributed to cell proliferation in the noncardiomyocyte fraction, given the limited capacity of the cardiomyocytes to reenter the cell cycle.[7] Herein, we explore whether osteopontin signaling could have an impact on

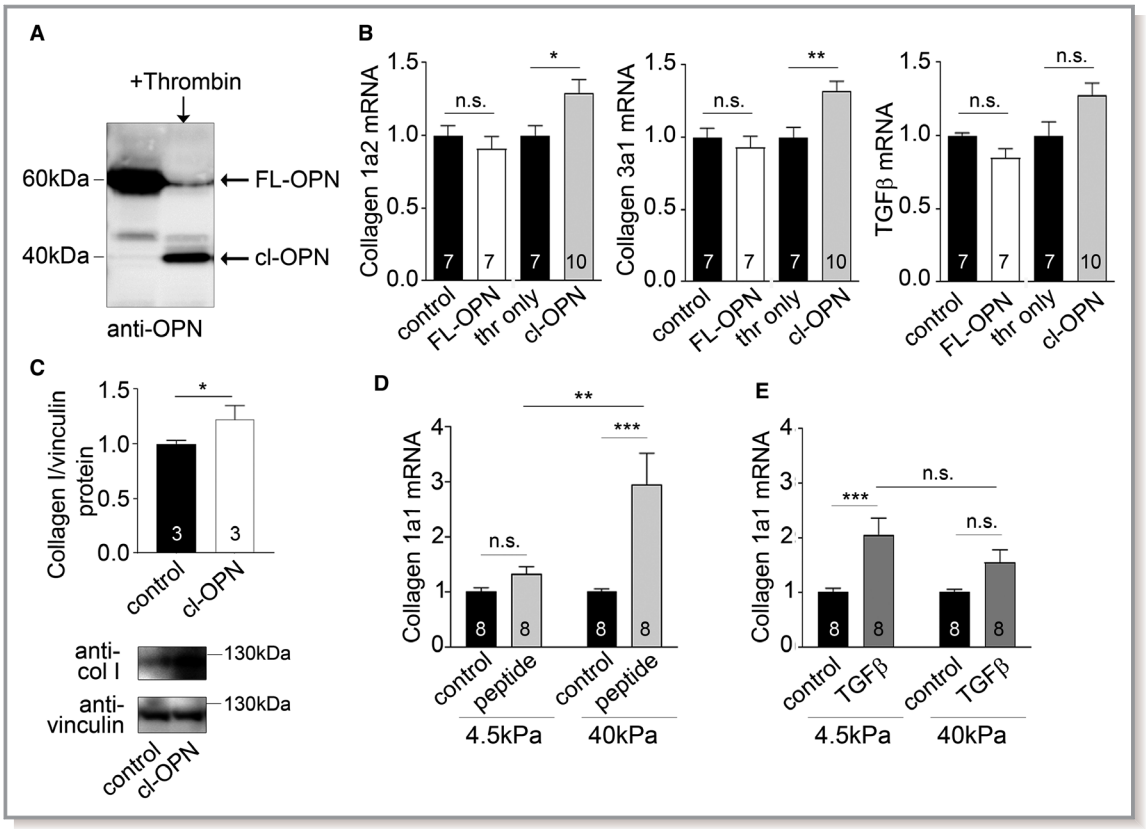

Figure 2. Thrombin-cleaved osteopontin (cl-OPN) increases collagen expression. **A**, Immunoblot of recombinant full-length osteopontin (FL-OPN) and cl-OPN. Expression of collagen 1a1, collagen 1a2, collagen 3a1, and transforming growth factor β 1 (TGFβ1) or collagen 1a1 promoter activation was measured in cardiac fibroblasts from wild-type (**B** through **E**, **H**, and **I**) and col1a1–GFP (green fluorescent protein) reporter mice (**F** and **G**), respectively. Cells were stimulated with FL-OPN, cl-OPN, thrombin, the RGDSLAYGLR peptide, and TGFβ for various time points (**F**), 24 hours (**B** through **E**, **H**, and **I**), or 9 hours (**G**). Neonatal cardiac fibroblasts were used in **B**, and adult cardiac fibroblasts were used in **C** through **I**. mRNA was normalized to GAPDH. Student *t* test was used to determine significant changes in **B**, **C**, and **I**. Two-way ANOVA was used to determine effect of gel stiffness (D*), peptide (D***, H**), TGFβ (E***), time (F***), stimulations (F***, G*), and SB431542 (G***, H***). Repeated-measures ANOVA was used in **F**. Interaction was significant for D*, G***, F***, and H***. Tukey's multiple comparisons test is indicated in each graph. SB431542-treated cells are compared with respective stimulations with TGFβ, peptide, or TGFβ+peptide. Numbers are indicated in graphs. $^{\#}P<0.05$, $^{\#\#}P<0.01$, $^{\#\#\#}P<0.005$. $^{\dagger}P<0.05$, $^{\dagger\dagger}P<0.01$, $^{\dagger\dagger\dagger}P<0.005$. n.s. indicates not significant.

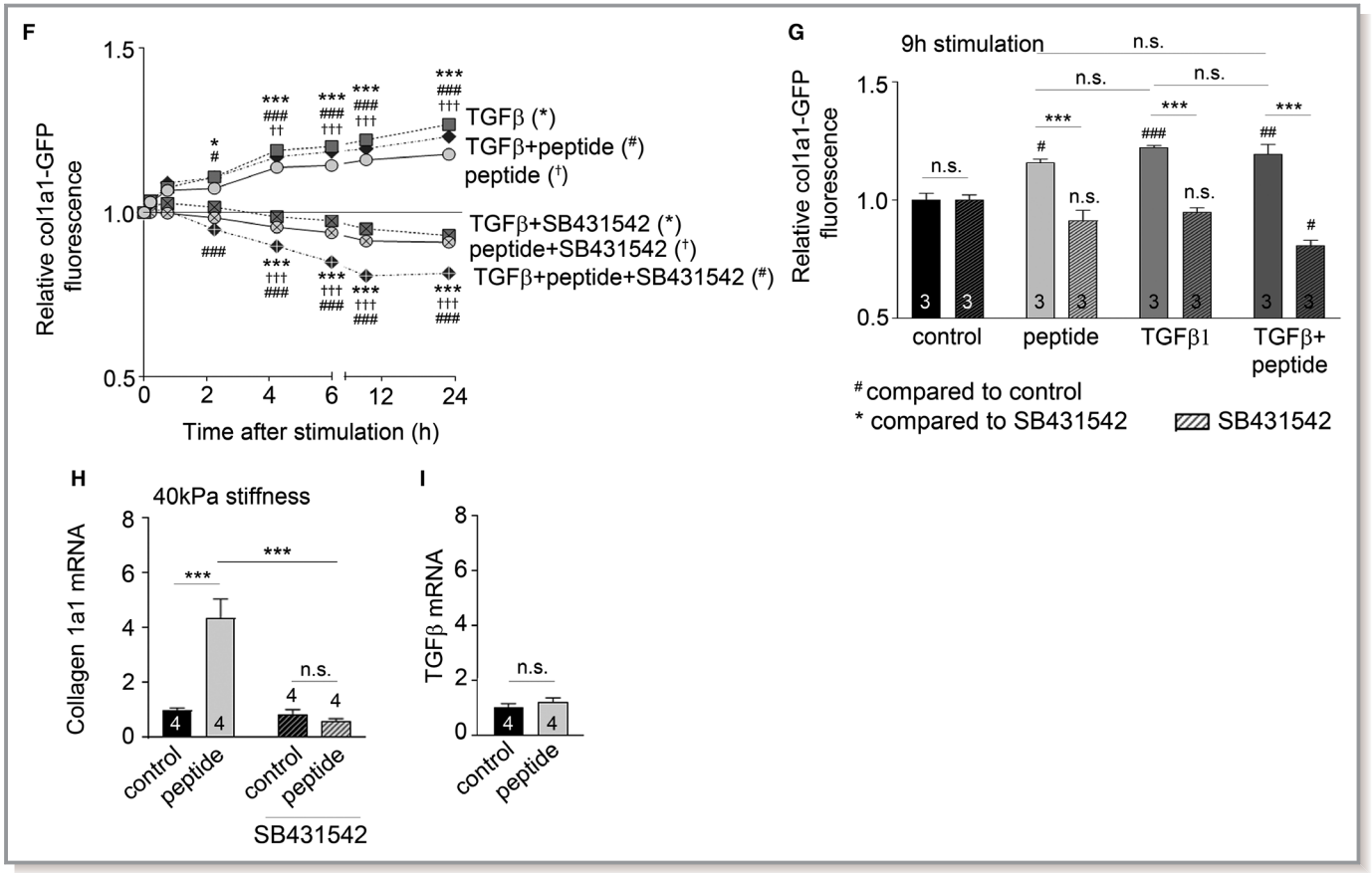

Figure 2. Continued.

cardiac fibroblast proliferation. We found that 24 hours of stimulation with cl-OPN increased mRNA levels of PCNA in primary cardiac fibroblasts and in HT1080 fibroblast (Figure S5A and S5C). FL-OPN had no impact on PCNA mRNA expression in cardiac fibroblasts but reduced PCNA protein levels in cardiac fibroblasts and PCNA mRNA expression in HT1080 fibroblasts (Figure S5A through S5C).

We plated cardiac fibroblasts on fibronectin-coated coverslips, a procedure we have previously shown to induce myofibroblast differentiation,[6] and tested the effects of FL-OPN and cl-OPN. No change in SMA fibers was observed for any of the stimulations (Figure S5D and S5E). At the same time point, we could not detect any impact on SMA and SM22 gene expression (Figure S5F and S5G). Furthermore, collagen 3a1, TGFβ, MMP2, and MMP9 mRNA were not affected by stimulation with the RGDSLAYGLR peptide (Figure S5H through S5K), suggesting that profibrotic effects of cl-OPN are mainly through collagen I synthesis.

Syndecan-4 Binds and Protects FL-OPN From Thrombin Cleavage

To test whether syndecan-4 binds FL-OPN in the heart and thereby alters osteopontin's susceptibility to thrombin cleavage, left ventricular lysates from WT and syndecan-4$^{-/-}$ mice were examined on 2 separate native PAGE and analyzed by immunoblotting using either an antibody specific to the unique V region in syndecan-4 cytoplasmic tail (epitope mapped by Finsen et al[27]) or anti-osteopontin. Both independent blots probed with each antibody showed a large protein complex just below the wells (Figure 3A and Figure S6A). Stripping and reprobing each Western blot with the other antibody confirmed that the 2 antibodies recognized the same protein complex (ie, blot Figure 3A: anti–syndecan-4, reprobed with anti-osteopontin; blot Figure S6A: anti-osteopontin, reprobed with anti–syndecan-4). The osteopontin–syndecan-4 complex was not detected in lysates from syndecan-4$^{-/-}$ mice, substantiating that syndecan-4 is necessary for the complex to form. Immunoprecipitation confirmed binding of osteopontin and syndecan-4 in cell lysates from NIH 3T3 fibroblasts (Figure 3B and Figure S6B) and from primary cardiac fibroblasts (Figure 3C and Figure S6C).

To test whether syndecan-4 binding could protect osteopontin from proteolytic cleavage by thrombin, recombinant FL-OPN was incubated with thrombin in the presence or absence of the extracellular domain of syndecan-4 (amino acids 1–146 with GAG chains). To our surprise, addition of syndecan-4 alone was not able to prevent thrombin cleavage

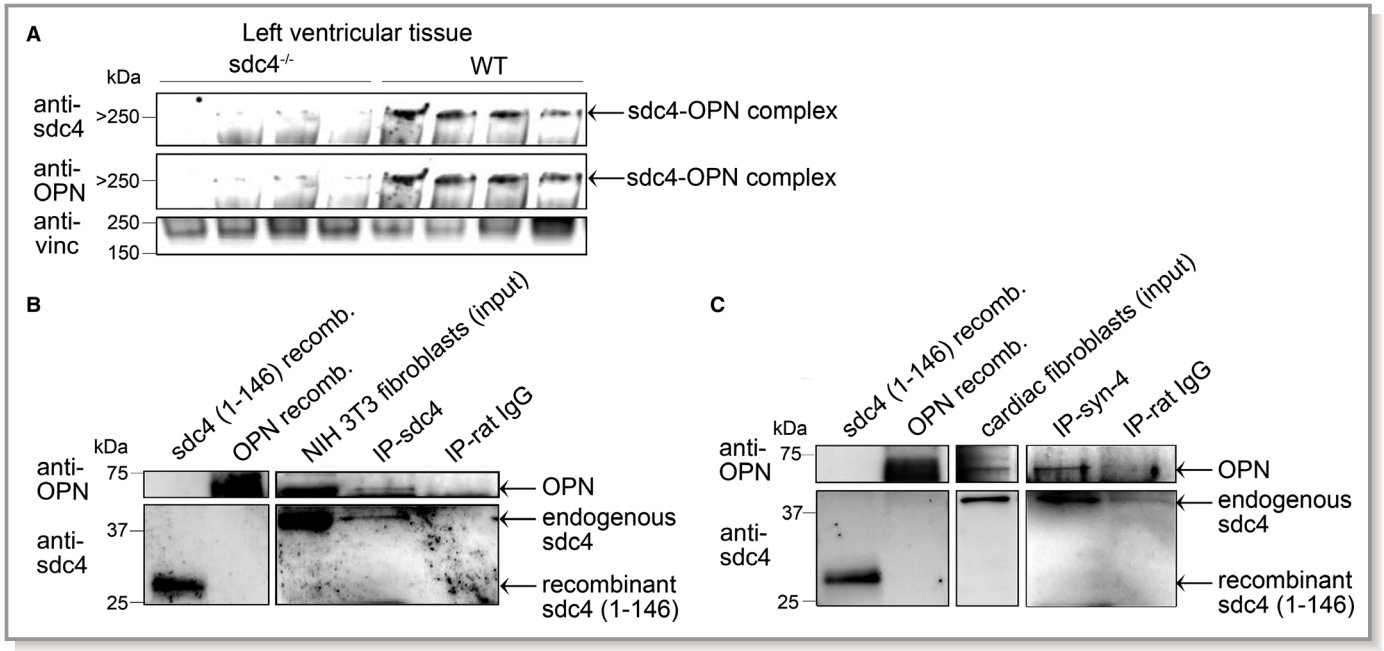

Figure 3. Syndecan-4 binds osteopontin in left ventricular tissue and cardiac fibroblasts. **A**, Detection of a syndecan-4–osteopontin high-molecular-weight complex in left ventricular homogenates from wild-type (WT) mice on native PAGE using anti–syndecan-4. Stripping and reprobing with anti-osteopontin confirmed that the 2 antibodies recognized the same protein complex in WT homogenates. The opposite probing order (anti-osteopontin, stripped and reprobed with anti–syndecan-4) is shown in Figure S5A. Left ventricle homogenate from syndecan-4 knockout mice was used as negative control (lanes 1–4). Vinculin was used as loading control. Immunoprecipitation of syndecan-4–osteopontin complex in cell lysates from NIH 3T3 fibroblasts (**B**) and primary neonatal cardiac fibroblasts from rat (**C**). Recombinant syndecan-4 (amino acids 1–146) and osteopontin proteins were used as positive controls for the immunoblotting.

of FL-OPN, but addition of syndecan-4 in the presence of 2 mmol/L Ca^{2+}, a concentration equivalent to that of the extracellular environment of the heart, resulted in significantly reduced thrombin cleavage of FL-OPN (Figure 4). Adding Ca^{2+} in the absence of syndecan-4 had no protective effect on thrombin cleavage (Figure S7).

Shedding of the Extracellular Domain of Syndecan-4 Increases in the Pressure-Overloaded Heart

In agreement with our previous work, syndecan-4 mRNA is significantly elevated days after AB.[6,7,31] Herein, we show that syndecan-4 expression is rapidly increased, already 1 hour after AB, peaking at 6 hours and remaining elevated at 24 hours, 3 days, and 7 days (Figure 5A). The 6-hour peak was preceded by an immediate increase in the cytokines interleukin-1β and tumor necrosis factor α 1 and 6 hours after AB (Figure S8). This is in line with our previous published work showing that, in addition to mechanical stress, syndecan-4 expression is induced by the early sterile inflammation caused by left ventricular pressure overload.[31] Syndecan-4 mRNA levels were also increased in myocardial biopsies from patients with aortic stenosis (Figure 5B).

The extracellular part of cardiac syndecan-4 can be shed off, and the degree of shedding was previously found to be increased in cardiac biopsies from patients with heart failure, as assessed by measurements of the cellular fragment of syndecan-4 remaining at the cell surface after shedding.[31] The extracellular shed fragment has been shown to be released to the circulation in patients with severe aortic stenosis.[40] Herein, we investigated the extent of syndecan-4 shedding in mice at various time points after AB. The extracellular shed fragment of syndecan-4 (15 kDa) relative to full-length syndecan-4 was slightly but significantly increased 24 hours after AB (Figure 5C). This modest degree of shedding is potentially induced by inflammatory cytokines that are increased at this early time point (Figure S8 and 31) and have been shown to induce shedding in vitro.[31] Seven days after AB, the ratio of shed/full-length syndecan-4 was substantially increased, remaining elevated 21 days after AB (Figure 5C). At this time point, expression of inflammatory cytokines had returned to baseline (Figure S8), and they were therefore less likely to be the main drivers of syndecan-4 shedding in late-phase remodeling. Because extracellular syndecan-4 protected osteopontin from thrombin cleavage (Figure 4), we explored whether shedding of cardiac syndecan-4 associated with increased cl-OPN in the pressure-overloaded

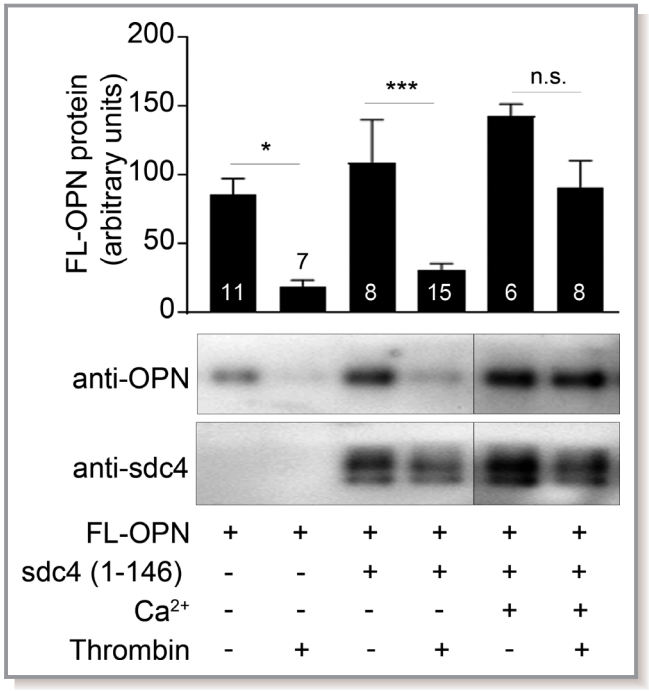

Figure 4. Syndecan-4 protects osteopontin from cleavage by thrombin in the presence of Ca^{2+}. Quantification and representative Western blot of recombinant full-length osteopontin (FL-OPN) protein levels after incubation with recombinant extracellular syndecan-4 (1–146), 2 mmol/L Ca^{2+}, and thrombin. One-way ANOVA with Holm-Sidak's multiple comparisons test, as indicated, was used to determine significant differences. Numbers are indicated in graphs. n.s. indicates not significant. *P<0.05, ***P<0.005.

heart. Interestingly, although FL-OPN was increased both at 24 hours and 21 days, cl-OPN was significantly increased at the later time point only (Figure 5D and 5E), a time point that coincides with higher extent of shedding. Antibody specificity to FL-OPN and cl-OPN was verified by immunoblotting with the primary antibody (ab181440) with and without the specific osteopontin blocking peptide (Figure S9). The sequence of the osteopontin blocking peptide is shown in Figure S1B.

Osteopontin can also be cleaved by other proteases, including MMP2, MMP3, MMP7, and MMP9, having cleavage sites distinct from the thrombin cleavage site.[19] Of these, MMP2, MMP3, and MMP9 mRNA were detected in left ventricular tissue lysates and were increased in response to pressure overload, albeit with temporal differences. MMP3, MMP9, and their tissue inhibitor of metalloproteinases (TIMP) 1 peaked 24 hours after AB (Figure S10A through S10C), whereas MMP2 and TIMP2 expression coincided with osteopontin cleavage reaching a peak 7 days after AB with continued elevation 21 days after AB (Figure S10D and S10E). Thus, MMP2 could potentially cleave osteopontin in the late remodeling phase.

Considering the in vitro stimulatory effects of cl-OPN on cardiac fibroblast gene expression depicted in Figure 2, collagen expression would be expected to increase in the absence of syndecan-4 by virtue of a reduced protection of osteopontin from thrombin cleavage. Indeed, mRNA expression of collagen 1a2 (Figure 5F) and 3a1 (Figure 5G) was higher in left ventricular tissue lysates from syndecan-$4^{-/-}$ mice compared with WT mice 21 days after AB. At this time point, echocardiography data show that left ventricular inner diameter is increased in the syndecan-$4^{-/-}$ compared with WT mice (Table S2), suggesting transition toward heart failure, which has previously been demonstrated in this knockout mouse to occur 4 weeks after AB.[27]

Discussion

We showed that osteopontin, in its full-length form, was increased in left ventricular tissue during the early phase after initiation of pressure overload in mice (schematically illustrated in the left panel in Figure 6). However, osteopontin did not induce collagen I expression unless it was cleaved by thrombin. We also demonstrate that FL-OPN binds to the extracellular part of syndecan-4 at physiological levels of Ca^{2+} and that this binding protects FL-OPN from cleavage by thrombin. Syndecan-4 is present on the cell surface at high levels in the early remodeling phase after AB, but the extracellular domain of syndecan-4 is shed in the late remodeling phase in mice, an event that triggers enhanced thrombin cleavage of osteopontin (schematically illustrated in the right panel in Figure 6). On cleavage by thrombin, a specific peptide sequence on the N-terminal fragment of cl-OPN is exposed (RGDSLAYGLR). Treating cardiac fibroblasts with cl-OPN or this specific peptide sequence induced collagen 1a1 expression, supporting that cl-OPN clearly has the potential to promote progression of cardiac fibrosis in vivo (Figure 6, right panel).

Osteopontin expression was substantially upregulated in the early phase of remodeling after AB. Others have also shown increased osteopontin expression after left ventricular pressure overload in rats and mice and suggested it to have profibrotic capacity.[41–43] However, herein, we demonstrated that it is not the FL-OPN, but the cl-OPN, that has profibrotic activity. Like osteopontin, we have previously shown that syndecan-4 is highly upregulated during the early remodeling phase and, in fact, regulates osteopontin gene expression via nuclear factor of activated T cell signaling.[7] Our data indicate that the high level of syndecan-4 contributes to maintaining osteopontin in its full-length form in addition to regulating its expression.

We show that syndecan-4 binds to osteopontin in left ventricular tissue and in cardiac fibroblast cultures, thereby protecting osteopontin from cleavage by thrombin. This binding was dependent on the presence of Ca^{2+} ions in a

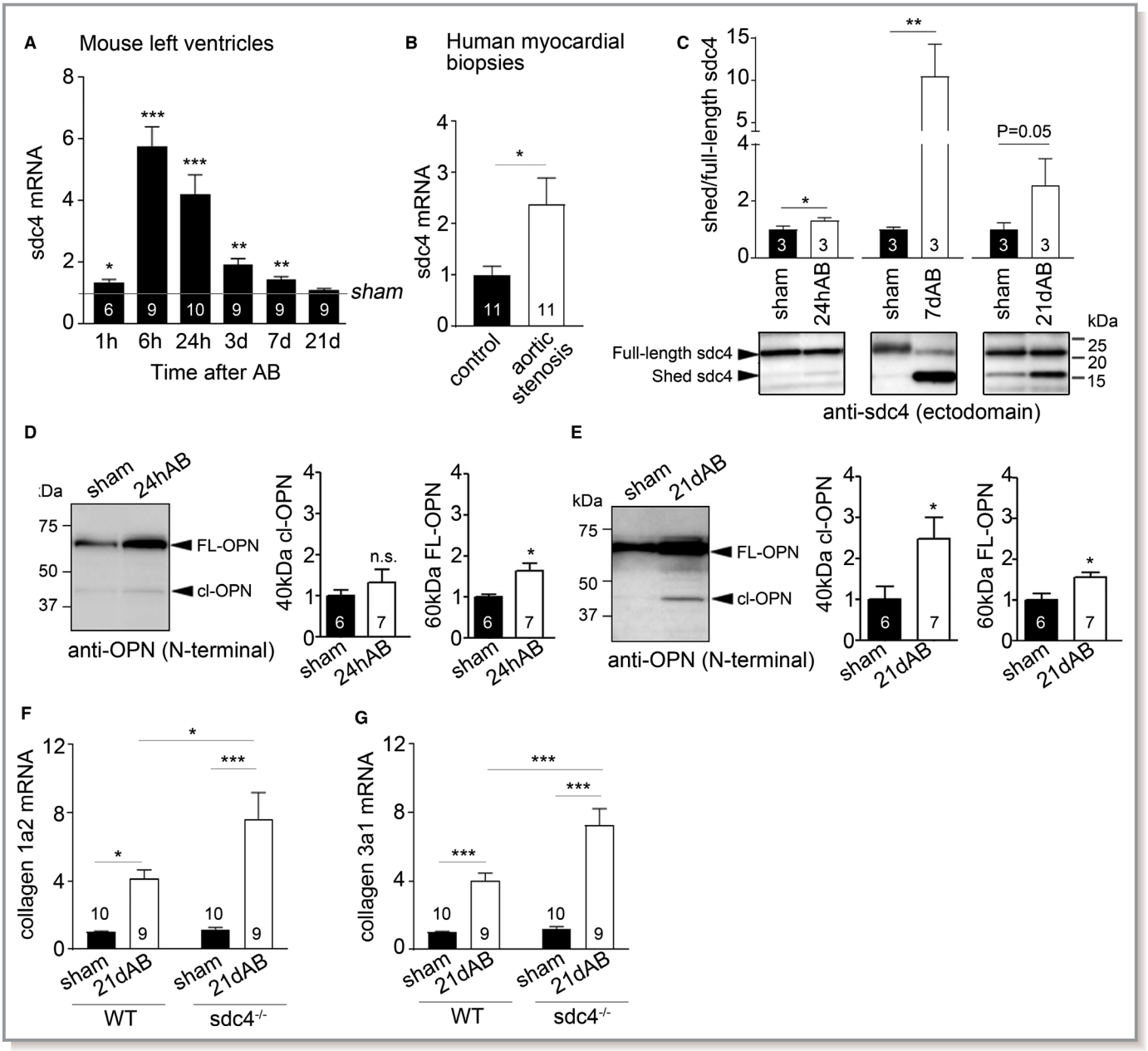

Figure 5. The extracellular domain of syndecan-4 is shed and cleavage of osteopontin is increased during advanced stages of extracellular matrix remodeling after pressure overload. **A**, Left ventricular syndecan-4 mRNA at different time points after aortic banding (AB). The line indicates sham levels. The 24-hour, 7-day, and 21-day time points were previously published.[40] **B**, Syndecan-4 mRNA in myocardial biopsies from patients with aortic stenosis. **C**, Immunoblot (**bottom panel**) and quantification (**top panel**) of the 15-kDa extracellular syndecan-4 fragment representing the shed ectodomain and full-length syndecan-4 (20–25 kDa) in myocardium after 24 hours, 7 days, and 21 days of AB. **D** and **E**, Immunoblot and quantification of full-length osteopontin (FL-OPN) and thrombin-cleaved osteopontin (cl-OPN) after 24 hours (**D**) and 21 days (**E**) of AB. Collagen 1a2 (**F**) and collagen 3a1 (**G**) mRNA expression in left ventricular tissue lysate from wild-type (WT) and syndecan-4 knockout mice subjected to 21 days of AB. mRNA levels were normalized to GAPDH for mouse samples and to Rpl32 for human samples. Student *t* test was used to determine significant differences in **A** through **E**. Two-way ANOVA with Tukey's multiple comparisons test was used to determine significant differences in **F** and **G**. Numbers are indicated in graphs. n.s. indicates not significant. **P*<0.05, ***P*<0.01, ****P*<0.005.

concentration corresponding to that of the extracellular compartment in the heart. Osteopontin has a Ca^{2+}-binding domain[44] that may be needed to facilitate binding to the heparan sulfate chains of syndecan-4. Alternatively, the binding may be of ionic nature because the glycosaminoglycan chains of syndecan-4 are highly negatively charged. Because the net charge of osteopontin also is negative, the positively charged Ca^{2+} ions may function to promote ionic binding or cancel ionic repulsive forces between osteopontin and syndecan-4.

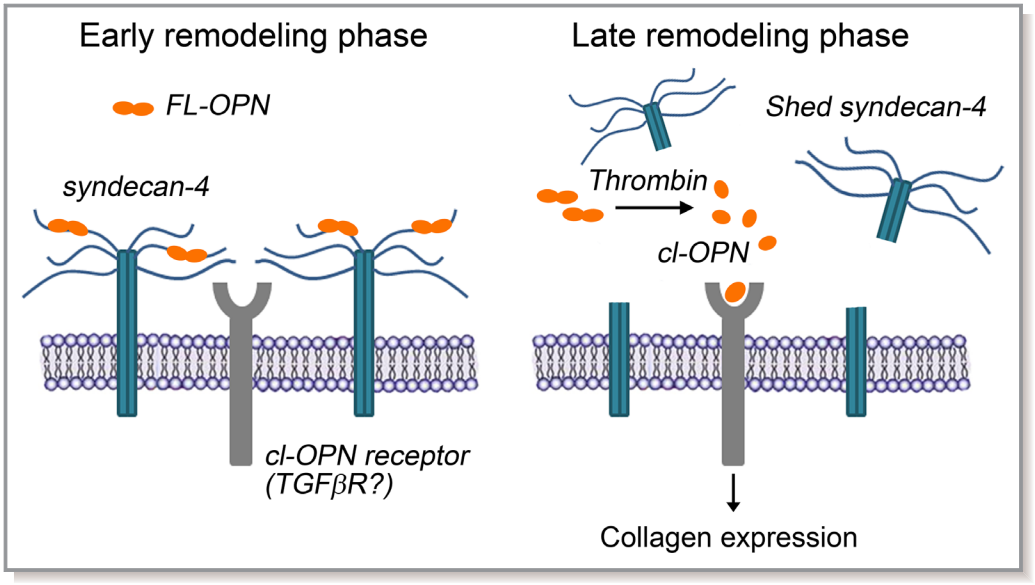

Figure 6. Syndecan-4 protects osteopontin from cleavage by thrombin, thereby preventing osteopontin-induced profibrotic collagen production. Osteopontin is immediately upregulated in left ventricular tissue after inducing pressure overload by aortic banding. In this early remodeling phase, syndecan-4 is also highly upregulated. Osteopontin binds to the extracellular part of syndecan-4, thereby becoming protected from cleavage by thrombin that enters the myocardial tissue from the circulation. At later phases of remodeling, the extracellular part of syndecan-4 is shed, and the protective effect on osteopontin cleavage is lost. The resulting cleaved osteopontin fragment induces profibrotic collagen expression via transforming growth factor β receptor (TGFβR) signaling, thereby promoting fibrosis. cl-OPN indicates thrombin-cleaved osteopontin; FL-OPN, full-length osteopontin.

In agreement with results from failing human hearts,[31] we show that syndecan-4 is shed in late-phase remodeling after AB, at which time cl-OPN was increased in the myocardium. Shed syndecan-4 is, in part, removed into the bloodstream, where it can be detected in patients with aortic stenosis,[40] acute myocardial infarction,[45] and chronic heart failure.[46] Consequently, reduced extracellular syndecan-4 in the myocardium exposes osteopontin to cleavage by thrombin. Interestingly, thrombin itself has been reported to shed syndecan-4.[47] Hence, it is possible that thrombin first sheds off syndecan-4 ectodomain and subsequently cleaves osteopontin if tissue damage and thrombin activity persist.

cl-OPN and the RGDSLAYGLR peptide induced collagen I expression, the most abundant collagen in the heart and crucial for fibrosis development. This response was only present when cardiac fibroblasts were cultured on stiff gels or plastic, indicating more potent effect of cl-OPN in the late phase of cardiac remodeling when some myocardial stiffening has occurred. The regulation of collagen gene expression by cl-OPN is in agreement with recent reports showing upregulation of collagen I[20] and collagen III[23] in response to cl-OPN or the human SVVYGLR peptide (corresponding to mouse SLAYGLR peptide). Thus, blocking osteopontin cleavage or the cl-OPN fragment itself may be a potential intervention for preventing excessive collagen accumulation at later stages of remodeling.

Interestingly, the TGFβRI inhibitor SB431542 blocked upregulation of collagen 1a1 by the RGDSLAYGLR peptide, suggesting that cl-OPN uses the TGFβ signaling pathway to induce fibrosis. Correspondingly, the peptide sequence SVVYGLR was recently found to bind directly to the TGFβR,[48] and blocking this receptor inhibited activation of the Smad signaling pathway induced by the osteopontin-derived peptide.[23] In contrast to cl-OPN, the effect of TGFβ on collagen expression was only present in cardiac fibroblasts plated on soft gels with a stiffness resembling that of the myocardium during early remodeling. Taken together, these results indicate that signaling via the TGFβR is initiated by TGFβ in the early phase, whereas cl-OPN is a more potent ligand for TGFβR in the more advanced phases of remodeling.

Osteopontin was cleaved by thrombin in left ventricular tissue of the pressure-overloaded murine and human heart. Recently, thrombin was found to be upregulated in the myocardium of patients with heart failure,[15] supporting the possibility that increased thrombin in pressure-overloaded human hearts may be cardiac derived. However, we did not detect thrombin mRNA in left ventricular tissue homogenates of sham and AB WT mice, suggesting that thrombin may enter the interstitial space from the bloodstream through leaky vessels or in areas of tissue damage, where it has the capacity to cleave osteopontin and thereby induce activation of cardiac

fibroblasts to promote tissue repair. This hypothesis would suggest that cl-OPN acts in the proximity to blood vessels, thus affecting pressure overload-induced perivascular fibrosis. Indeed, immunostaining of cl-OPN indicated accumulation along blood vessels.

Along these lines, inhibition of thrombin has been reported to reduce fibrosis and improve diastolic function without affecting cardiomyocyte hypertrophy 5 weeks after transaortic constriction. Whether this inhibition targeted interstitial or perivascular fibrosis was not specified.[24]

Genetically modified mice lacking osteopontin have provided valuable insight into the role of cardiac osteopontin for cardiac fibrosis and diastolic function after myocardial infarction,[49] aldosterone infusion,[50] and AB.[42] However, because of the multifaceted nature of osteopontin, the cardiac phenotype of total osteopontin deletion may obscure important roles of osteopontin because its function also depends on cellular location and proteolytic cleavage.[17,51,52] This is clearly demonstrated in our in vitro experiments showing dissimilar and opposite effects of FL-OPN and cl-OPN on cardiac fibroblast phenotype and profibrotic activity. Furthermore, lack of the intracellular form of osteopontin is presumably responsible for the impaired TGFβ-induced myofibroblast differentiation of cardiac fibroblasts from osteopontin knockout mice.[17] We did not see induction but rather inhibition of myofibroblast differentiation in response to extracellular FL-OPN, thus underscoring the importance of distinguishing between effects of different osteopontin variants.

Studies on liver fibrosis have shown that extracellular syndecan-4 administration protects mice from inflammation-induced hepatic injury by inhibiting osteopontin cleavage.[10] A similar approach in the heart could potentially be exploited as antifibrotic therapy for the heart. Indeed, mice treated with an RNA aptamer to block osteopontin signaling had reduced cardiac fibrosis after inducing pressure overload,[18] and profibrotic gene expression was enhanced in the late phase of remodeling and was associated with accelerated transition to heart failure in mice lacking syndecan-4.[27] Furthermore, it is important to consider the dual role of ECM production for cardiac function: Some ECM production is necessary to prevent cardiac rupture during myocardial infarction and enable recovery of structural stability during the adaption to higher pressures. On the other hand, excessive ECM production will cause diastolic dysfunction because of the reduced ability of the heart to distend during diastole. Hence, temporal specificity of antifibrotic treatment is necessary. Targeting profibrotic signals present in late-stage remodeling, such as cl-OPN, might be an attractive approach.

In conclusion, we show that syndecan-4 protects osteopontin from cleavage by thrombin in the early phase of pressure overload-induced cardiac remodeling. This protection is lost when syndecan-4 is shed from the cell surface in later phases of remodeling, thereby promoting the progression of cardiac fibrosis.

Acknowledgments

The authors would like to thank David Brenner for kindly providing the col1a1 (Collagen 1a1)–GFP (green fluorescent protein) reporter mouse. The authors are grateful for the technical assistance of Dina Behmen, Almira Hasic, Jennifer Stowe, Marianne Lunde, and Biljana Skrbic. Moreover, thanks to the anesthesiologists and surgeons at the Department of Cardiothoracic Surgery, Oslo University Hospital (Ullevål, Norway) for helping with obtaining human blood samples.

Sources of Funding

The authors are grateful for the funding from The Research Council of Norway (Dr Herum) and the European Commission Marie Curie Actions' COFUND Program (Dr Herum). This work was supported in part by the National Institutes of Health via grants GM094503, GM103426, HL105242, HL122199, and HL105242, and California Institute of Regenerative Medicine grant CIRM RT3-07899. This work was also funded by grants from the Swedish Research Council (No. 2018-02837; EXODIAB No. 2009-1039), the Swedish Heart and Lung Foundation (No. 20160872), and the Swedish Foundation for Strategic Research (LUDC-IRC No. 15-0067) to Dr Gomez.

Disclosures

Dr McCulloch is a cofounder, scientific advisor, and equity holder of Insilicomed, Inc, and a scientific advisor and cofounder of Vektor Medical, licensees of University of California, San Diego, software that was not used in this research. Insilicomed, Inc, and Vektor Medical had no involvement at all in design, performance, analysis, or funding of the present study. This relationship has been disclosed to, reviewed, and approved by the University of California, San Diego, in accordance with its conflict of interest policies. The remaining authors have no disclosures to report.

References

1. Porter KE, Turner NA. Cardiac fibroblasts: at the heart of myocardial remodeling. *Pharmacol Ther*. 2009;123:255–278.
2. Li L, Zhao Q, Kong W. Extracellular matrix remodeling and cardiac fibrosis. *Matrix Biol*. 2018;68–69:490–506.
3. Schaefer L. Decoding fibrosis: mechanisms and translational aspects. *Matrix Biol*. 2018;68–69:1–7.
4. Lunde IG, Herum KM, Carlson CC, Christensen G. Syndecans in heart fibrosis. *Cell Tissue Res*. 2016;365:539–552.
5. Christensen G, Herum KM, Lunde IG. Sweet, yet underappreciated: proteoglycans and extracellular matrix remodeling in heart disease. *Matrix Biol*. 2018;75–76:286–299.

6. Herum KM, Lunde IG, Skrbic B, Florholmen G, Behmen D, Sjaastad I, Carlson CR, Gomez MF, Christensen G. Syndecan-4 signaling via NFAT regulates extracellular matrix production and cardiac myofibroblast differentiation in response to mechanical stress. *J Mol Cell Cardiol*. 2013;54:73–81.
7. Herum KM, Lunde IG, Skrbic B, Louch WE, Hasic A, Boye S, Unger A, Brorson SH, Sjaastad I, Tønnessen T, Linke WA, Gomez MF, Christensen G. Syndecan-4 is a key determinant of collagen cross-linking and passive myocardial stiffness in the pressure-overloaded heart. *Cardiovasc Res*. 2015;106:217–226.
8. Rapraeger AC, Krufka A, Olwin BB. Requirement of heparan sulfate for bFGF-mediated fibroblast growth and myoblast differentiation. *Science*. 1991;252:1705–1708.
9. Slimani H, Charnaux N, Mbemba E, Saffar L, Vassy R, Vita C, Gattegno L. Interaction of RANTES with syndecan-1 and syndecan-4 expressed by human primary macrophages. *Biochim Biophys Acta*. 2003;1617:80–88.
10. Kon S, Ikesue M, Kimura C, Aoki M, Nakayama Y, Saito Y, Kurotaki D, Diao H, Matsui Y, Segawa T, Maeda M, Kojima T, Uede T. Syndecan-4 protects against osteopontin-mediated acute hepatic injury by masking functional domains of osteopontin. *J Exp Med*. 2008;205:25–33.
11. Xian X, Gopal S, Couchman JR. Syndecans as receptors and organizers of the extracellular matrix. *Cell Tissue Res*. 2010;339:31–46.
12. Lopez B, Gonzalez A, Lindner D, Westermann D, Ravassa S, Beaumont J, Gallego I, Zudaire A, Brugnolaro C, Querejeta R, Larman M, Tschope C, Diez J. Osteopontin-mediated myocardial fibrosis in heart failure: a role for lysyl oxidase? *Cardiovasc Res*. 2013;99:111–120.
13. Abdalrhim AD, Marroush TS, Austin EE, Gersh BJ, Solak N, Rizvi SA, Bailey KR, Kullo IJ. Plasma osteopontin levels and adverse cardiovascular outcomes in the PEACE Trial. *PLoS One*. 2016;11:e0156965.
14. Behnes M, Brueckmann M, Lang S, Espeter F, Weiss C, Neumaier M, Ahmad-Nejad P, Borggrefe M, Hoffmann U. Diagnostic and prognostic value of osteopontin in patients with acute congestive heart failure. *Eur J Heart Fail*. 2013;15:1390–1400.
15. Cabiati M, Svezia B, Matteucci M, Botta L, Pucci A, Rinaldi M, Caselli C, Lionetti V, Del Ry S. Myocardial expression analysis of osteopontin and its splice variants in patients affected by end-stage idiopathic or ischemic dilated cardiomyopathy. *PLoS One*. 2016;11:e0160110.
16. Frangogiannis NG. Matricellular proteins in cardiac adaptation and disease. *Physiol Rev*. 2012;92:635–688.
17. Lenga Y, Koh A, Perera AS, McCulloch CA, Sodek J, Zohar R. Osteopontin expression is required for myofibroblast differentiation. *Circ Res*. 2008;102:319–327.
18. Li J, Yousefi K, Ding W, Singh J, Shehadeh LA. Osteopontin RNA aptamer can prevent and reverse pressure overload-induced heart failure. *Cardiovasc Res*. 2017;113:633–643.
19. Lindsey ML, Zouein FA, Tian Y, Padmanabhan Iyer R, de Castro Bras LE. Osteopontin is proteolytically processed by matrix metalloproteinase 9. *Can J Physiol Pharmacol*. 2015;93:879–886.
20. Zhao H, Wang W, Zhang J, Liang T, Fan GP, Wang ZW, Zhang PD, Wang X, Zhang J. Inhibition of osteopontin reduce the cardiac myofibrosis in dilated cardiomyopathy via focal adhesion kinase mediated signaling pathway. *Am J Transl Res*. 2016;8:3645–3655.
21. Podzimkova J, Palecek T, Kuchynka P, Marek J, Danek BA, Jachymova M, Kalousova M, Zima T, Linhart A. Plasma osteopontin levels in patients with dilated and hypertrophic cardiomyopathy. *Herz*. 2017;44:347–353.
22. Rubis P, Wisniowska-Smialek S, Dziewiecka E, Rudnicka-Sosin L, Kozanecki A, Podolec P. Prognostic value of fibrosis-related markers in dilated cardiomyopathy: a link between osteopontin and cardiovascular events. *Adv Med Sci*. 2017;63:160–166.
23. Uchinaka A, Hamada Y, Mori S, Miyagawa S, Saito A, Sawa Y, Matsuura N, Yamamoto H, Kawaguchi N. SVVYGLR motif of the thrombin-cleaved N-terminal osteopontin fragment enhances the synthesis of collagen type III in myocardial fibrosis. *Mol Cell Biochem*. 2015;408:191–203.
24. Dong A, Mueller P, Yang F, Yang L, Morris A, Smyth SS. Direct thrombin inhibition with dabigatran attenuates pressure overload-induced cardiac fibrosis and dysfunction in mice. *Thromb Res*. 2017;159:58–64.
25. Braathen B, Tonnessen T. Cold blood cardioplegia reduces the increase in cardiac enzyme levels compared with cold crystalloid cardioplegia in patients undergoing aortic valve replacement for isolated aortic stenosis. *J Thorac Cardiovasc Surg*. 2010;139:874–880.
26. Echtermeyer F, Streit M, Wilcox-Adelman S, Saoncella S, Denhez F, Detmar M, Goetinck P. Delayed wound repair and impaired angiogenesis in mice lacking syndecan-4. *J Clin Invest*. 2001;107:R9–R14.
27. Finsen AV, Lunde IG, Sjaastad I, Østli EK, Lyngra M, Jarstadmarken HO, Hasic A, Nygard S, Wilcox-Adelman SA, Goetinck PF, Lyberg T, Skrbic B, Florholmen G, Tønnessen T, Louch WE, Djurovic S, Carlson CR, Christensen G. Syndecan-4 is essential for development of concentric myocardial hypertrophy via stretch-induced activation of the calcineurin-NFAT pathway. *PLoS One*. 2011;6:e28302.
28. Krempen K, Grotkopp D, Hall K, Bache A, Gillan A, Rippe RA, Brenner DA, Breindl M. Far upstream regulatory elements enhance position-independent and uterus-specific expression of the murine alpha1(I) collagen promoter in transgenic mice. *Gene Expr*. 1999;8:151–163.
29. Moore-Morris T, Guimaraes-Camboa N, Banerjee I, Zambon AC, Kisseleva T, Velayoudon A, Stallcup WB, Gu Y, Dalton ND, Cedenilla M, Gomez-Amaro R, Zhou B, Brenner DA, Peterson KL, Chen J, Evans SM. Resident fibroblast lineages mediate pressure overload-induced cardiac fibrosis. *J Clin Invest*. 2014;124:2921–2934.
30. Yata Y, Scanga A, Gillan A, Yang L, Reif S, Breindl M, Brenner DA, Rippe RA. DNase I-hypersensitive sites enhance alpha1(I) collagen gene expression in hepatic stellate cells. *Hepatology*. 2003;37:267–276.
31. Strand ME, Herum KM, Rana ZA, Skrbic B, Askevold ET, Dahl CP, Vistnes M, Hasic A, Kvaløy H, Sjaastad I, Carlson CR, Tønnessen T, Gullestad L, Christensen G, Lunde IG. Innate immune signaling induces expression and shedding of the heparan sulfate proteoglycan syndecan-4 in cardiac fibroblasts and myocytes, affecting inflammation in the pressure-overloaded heart. *FEBS J*. 2013;280:2228–2247.
32. Frank R, Overwin H. SPOT synthesis: epitope analysis with arrays of synthetic peptides prepared on cellulose membranes. *Methods Mol Biol*. 1996;66:149–169.
33. Herum KM, Choppe J, Kumar A, Engler AJ, McCulloch AD. Mechanical regulation of cardiac fibroblast pro-fibrotic phenotypes. *Mol Biol Cell*. 2017;28:1871–1882.
34. Tse JR, Engler AJ. Preparation of hydrogel substrates with tunable mechanical properties. *Curr Protoc Cell Biol*. 2010;Chapter 10:Unit 10.16.
35. Snead AN, Insel PA. Defining the cellular repertoire of GPCRs identifies a profibrotic role for the most highly expressed receptor, protease-activated receptor 1, in cardiac fibroblasts. *FASEB J*. 2012;26:4540–4547.
36. Herum KM, Lunde IG, McCulloch AD, Christensen G. The soft- and hard-heartedness of cardiac fibroblasts: mechanotransduction signaling pathways in fibrosis of the heart. *J Clin Med*. 2017;6:E53.
37. Berry MF, Engler AJ, Woo YJ, Pirolli TJ, Bish LT, Jayasankar V, Morine KJ, Gardner TJ, Discher DE, Sweeney HL. Mesenchymal stem cell injection after myocardial infarction improves myocardial compliance. *Am J Physiol Heart Circ Physiol*. 2006;290:H2196–H2203.
38. Engler AJ, Carag-Krieger C, Johnson CP, Raab M, Tang HY, Speicher DW, Sanger JW, Sanger JM, Discher DE. Embryonic cardiomyocytes beat best on a matrix with heart-like elasticity: scar-like rigidity inhibits beating. *J Cell Sci*. 2008;121:3794–3802.
39. Gubbiotti MA, Vallet SD, Ricard-Blum S, Iozzo RV. Decorin interacting network: a comprehensive analysis of decorin-binding partners and their versatile functions. *Matrix Biol*. 2016;55:7–21.
40. Strand ME, Aronsen JM, Braathen B, Sjaastad I, Kvaløy H, Tønnessen T, Christensen G, Lunde IG. Shedding of syndecan-4 promotes immune cell recruitment and mitigates cardiac dysfunction after lipopolysaccharide challenge in mice. *J Mol Cell Cardiol*. 2015;88:133–144.
41. Singh K, Sirokman G, Communal C, Robinson KG, Conrad CH, Brooks WW, Bing OH, Colucci WS. Myocardial osteopontin expression coincides with the development of heart failure. *Hypertension*. 1999;33:663–670.
42. Xie Z, Singh M, Singh K. Osteopontin modulates myocardial hypertrophy in response to chronic pressure overload in mice. *Hypertension*. 2004;44:826–831.
43. Zhao M, Chow A, Powers J, Fajardo G, Bernstein D. Microarray analysis of gene expression after transverse aortic constriction in mice. *Physiol Genomics*. 2004;19:93–105.
44. Scatena M, Liaw L, Giachelli CM. Osteopontin: a multifunctional molecule regulating chronic inflammation and vascular disease. *Arterioscler Thromb Vasc Biol*. 2007;27:2302–2309.
45. Kojima T, Takagi A, Maeda M, Segawa T, Shimizu A, Yamamoto K, Matsushita T, Saito H. Plasma levels of syndecan-4 (ryudocan) are elevated in patients with acute myocardial infarction. *Thromb Haemost*. 2001;85:793–799.
46. Takahashi R, Negishi K, Watanabe A, Arai M, Naganuma F, Ohyama Y, Kurabayashi M. Serum syndecan-4 is a novel biomarker for patients with chronic heart failure. *J Cardiol*. 2011;57:325–332.
47. Subramanian SV, Fitzgerald ML, Bernfield M. Regulated shedding of syndecan-1 and -4 ectodomains by thrombin and growth factor receptor activation. *J Biol Chem*. 1997;272:14713–14720.

48. Uchinaka A, Kawaguchi N, Hamada Y, Mori S, Miyagawa S, Saito A, Sawa Y, Matsuura N. Transplantation of myoblast sheets that secrete the novel peptide SVVYGLR improves cardiac function in failing hearts. *Cardiovasc Res*. 2013;99:102–110.

49. Trueblood NA, Xie Z, Communal C, Sam F, Ngoy S, Liaw L, Jenkins AW, Wang J, Sawyer DB, Bing OH, Apstein CS, Colucci WS, Singh K. Exaggerated left ventricular dilation and reduced collagen deposition after myocardial infarction in mice lacking osteopontin. *Circ Res*. 2001;88:1080–1087.

50. Sam F, Xie Z, Ooi H, Kerstetter DL, Colucci WS, Singh M, Singh K. Mice lacking osteopontin exhibit increased left ventricular dilation and reduced fibrosis after aldosterone infusion. *Am J Hypertens*. 2004;17:188–193.

51. Weber GF, Zawaideh S, Hikita S, Kumar VA, Cantor H, Ashkar S. Phosphorylation-dependent interaction of osteopontin with its receptors regulates macrophage migration and activation. *J Leukoc Biol*. 2002;72:752–761.

52. Denhardt DT, Noda M, O'Regan AW, Pavlin D, Berman JS. Osteopontin as a means to cope with environmental insults: regulation of inflammation, tissue remodeling, and cell survival. *J Clin Invest*. 2001;107:1055–1061.

SUPPLEMENTAL MATERIAL

Table S1. Aorta stenosis patient characteristics.

Characteristics	All patients	Blood cardioplegia	Crystalloid cardioplegia
N	28	13	15
Age, y	69.6 ± 2.2	67.5 ± 2.2	71.5 ± 2.5
Female sex, no.	11	4	7
Extracorporeal circulation, min	103.7 ± 3.8	103.7 ± 4.3	103.7 ± 4.2
Crossclamp time, min	73.5 ± 4.0	76.2 ± 4.7	71.2 ± 4.3
Preoperative creatinin, µmol/L	78.5 ± 3.8	80.5 ± 4.0	76.7 ± 4.5
Max CK-MB, µg/L	41.9 ± 8.6	30.0 ± 2.2	52.1 ± 12.2
Max Troponin T, µg/L	0.85 ± 0.17	0.60 ± 0.10	1.06 ± 0.23
IVSd, cm	1.37 ± 0.07	1.35 ± 0.06	1.38 ± 0.09
Preoperative EF > 50%, no.	28	13	15

IVSd, interventricular septal thickness at end-diastole; EF, ejection fraction; CK-MB, creatine kinase isoenzyme MB. Data are presented as mean ± S.E.M. Max CK-MB and Max Troponin T levels have previously been shown to be significantly higher in patients receiving crystalloid compared to blood cardioplegia with a sample size of 80 patients[1], however, in this small subset of patients differences did not reach significance using Student's *t*-test (Max CK-MB, p = 0.1; and Max Troponin T, p = 0.1).

Table S2. Mice lacking syndecan-4 have thinner walls and larger inner diameter 21 days after aortic banding.

	Sham		AB	
	WT	Sdc4$^{-/-}$	WT	Sdc4$^{-/-}$
BW, g	26.35 ± 0.49 (10)	25.90 ± 0.49 (10)	23.85 ± 0.61 (10) ††	24.75 ± 0.47 (10)
TL, mm	17.98 ± 0.12 (10)	17.68 ± 0.20 (10)	17.48 ± 0.15 (10)	17.24 ± 0.22 (10)
LVW/TL, mg/mm	5.24 ± 0.18 (10)	4.68 ± 0.50 (10)	8.91 ± 0.17 (10) †††	8.90 ± 0.21 (10) †††
LW/TL, mg/mm	8.99 ± 0.15 (10)	8.69 ± 0.29 (10)	21.19 ± 1.58 (10) †††	20.31 ± 2.23 (10) †††
LAD, mm	1.88 ± 0.11 (7)	1.89 ± 0.33 (6)	3.30 ± 0.14 (6) †††	3.34 ± 0.11 (7) †††
IVSd, mm	0.55 ± 0.03 (7)	0.57 ± 0.05 (6)	1.01 ± 0.05 (6) †††	0.89 ± 0.04 (7) †††
LVPWd, mm	0.53 ± 0.03 (7)	0.64 ± 0.04 (6)	1.02 ± 0.04 (6) †††	0.98 ± 0.05 (7) †††
LVIDd, mm	4.34 ± 0.09 (7)	4.15 ± 0.12 (6)	4.00 ± 0.09 (6)	4.53 ± 0.19 (7) *
LVFS, %	19.65 ± 0.92 (7)	18.75 ± 1.88 (6)	14.20 ± 1.66 (6)	9.84 ± 1.71 (7) ††
E/E´	39.09 ± 2.25 (7)	45.22 ± 2.94 (6)	59.12 ± 6.02 (6) ††	52.27 ± 3.92 (7)

Echocardiography revealed significant differences between wild-type (WT) and syndecan-4$^{-/-}$ (Sdc4$^{-/-}$) mice subjected to aortic banding (AB). Significant differences were determined by two-way ANOVA with Tukey's post-hoc test as indicated with * for differences between WT and Sdc4$^{-/-}$ and † for differences between sham and AB. BW, body weight; TL, tibia length; LVW, left ventricular weight; LW, lung weight; LAD, left atrial diameter; IVSd, end diastolic interventricular septum thickness; LVPWd, end diastolic left ventricular posterior wall thickness; LVIDd, end diastolic left ventricular internal diameter; LVFS, left ventricular fractional shortening; E, early mitral inflow velocity; E´, early mitral annular velocity**.** Data are presented as mean ± S.E.M.

Figure S1. Epitope mapping of OPN antibodies.

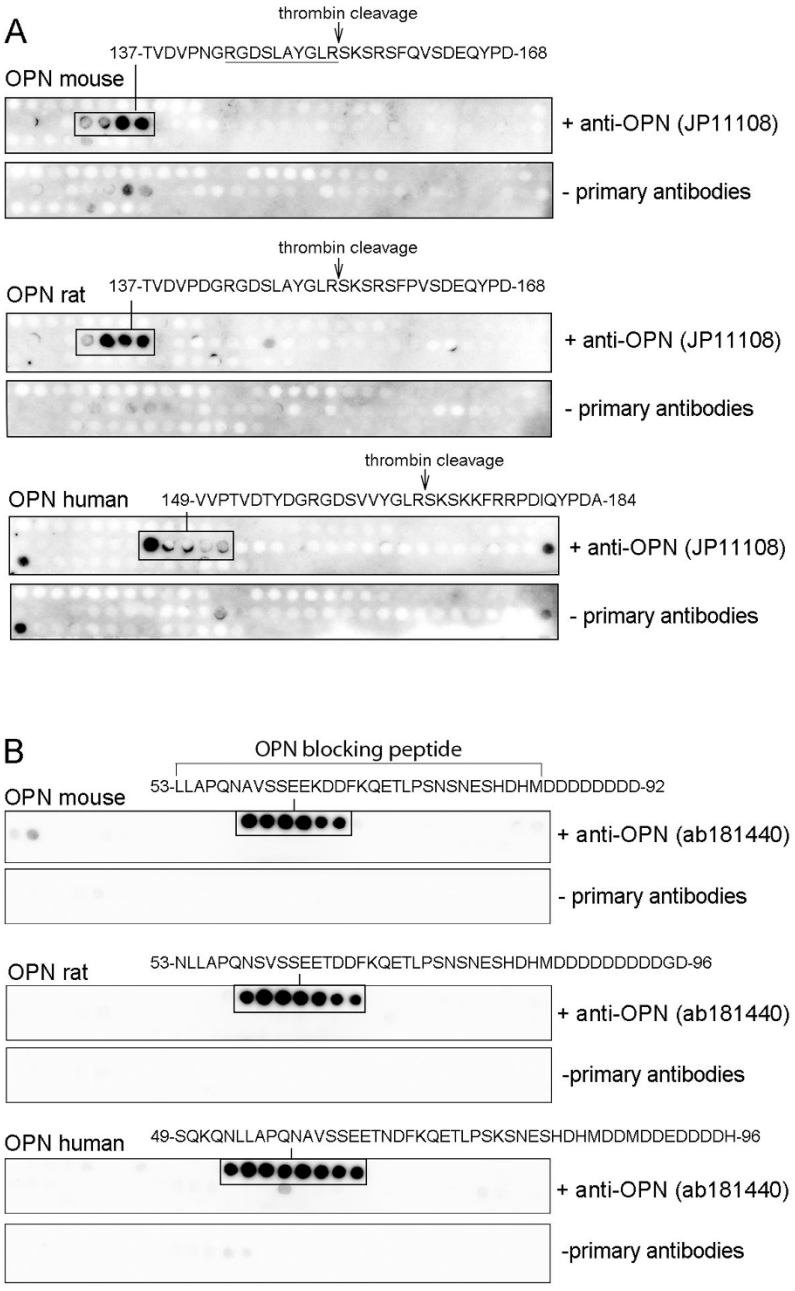

(A) anti-OPN (IBL, JP11108) or (B) anti-OPN (ab181440) were overlaid arrays of immobilized overlapping 20-mer peptides covering the mouse, rat or human OPN protein sequence. The given sequences above the arrays are relevant for antibody binding (n=2, two independent peptide array

syntheses). Immunoblotting without any primary antibodies were used as negative controls (lower panels in A-B). The thrombin cleavage site is indicated in the mouse, rat and human OPN sequences in A. The peptide sequence RGDSLAYGLR, used to stimulate cardiac fibroblasts, is underlined in mouse OPN in upper panel in A. Sequence of the OPN blocking peptide is shown in upper panel in B (mouse OPN, ab181440).

Figure S2. Micrographs of negative controls where primary antibodies were omitted.

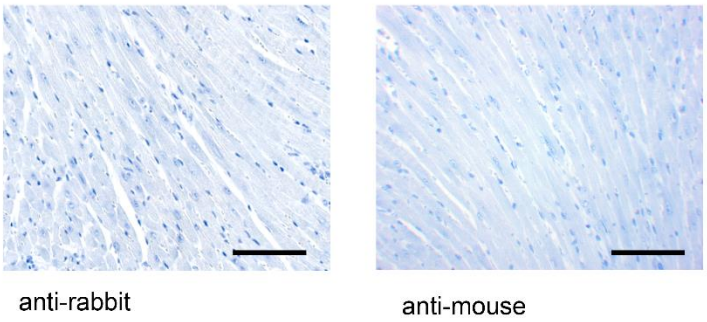

Scale bar 100 µm.

Figure S3. Osteopontin cleavage is higher in patients receiving crystalloid cardioplegia. in human plasma.

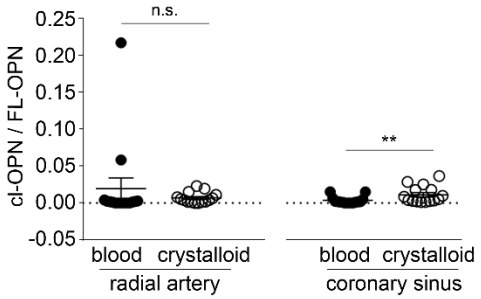

Ratio of cleaved osteopontin (cl-OPN) / full-length osteopontin (FL-OPN) in blood from the coronary sinus and radial artery of aortic stenosis (AS) patients receiving blood cardioplegia or crystalloid cardioplegia. Mann-Whitney test was used to determine significant changes. N = 15.

Figure S4. Cardiac expression of TGFβ and its natural inhibitor decorin.

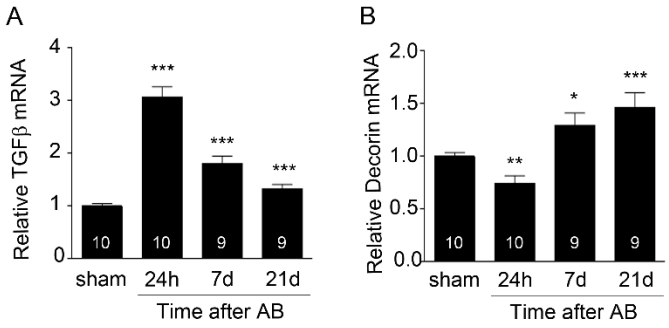

(A) Transforming growth factor b (TGFβ) and decorin mRNA levels in left ventricular tissue following aortic banding (AB). Student's t-test was used to determine significant differences between AB and corresponding sham (24 h sham shown in graph) for each time point. N are indicated in graphs.

Figure S5. Effect of osteopontin on cardiac fibroblasts.

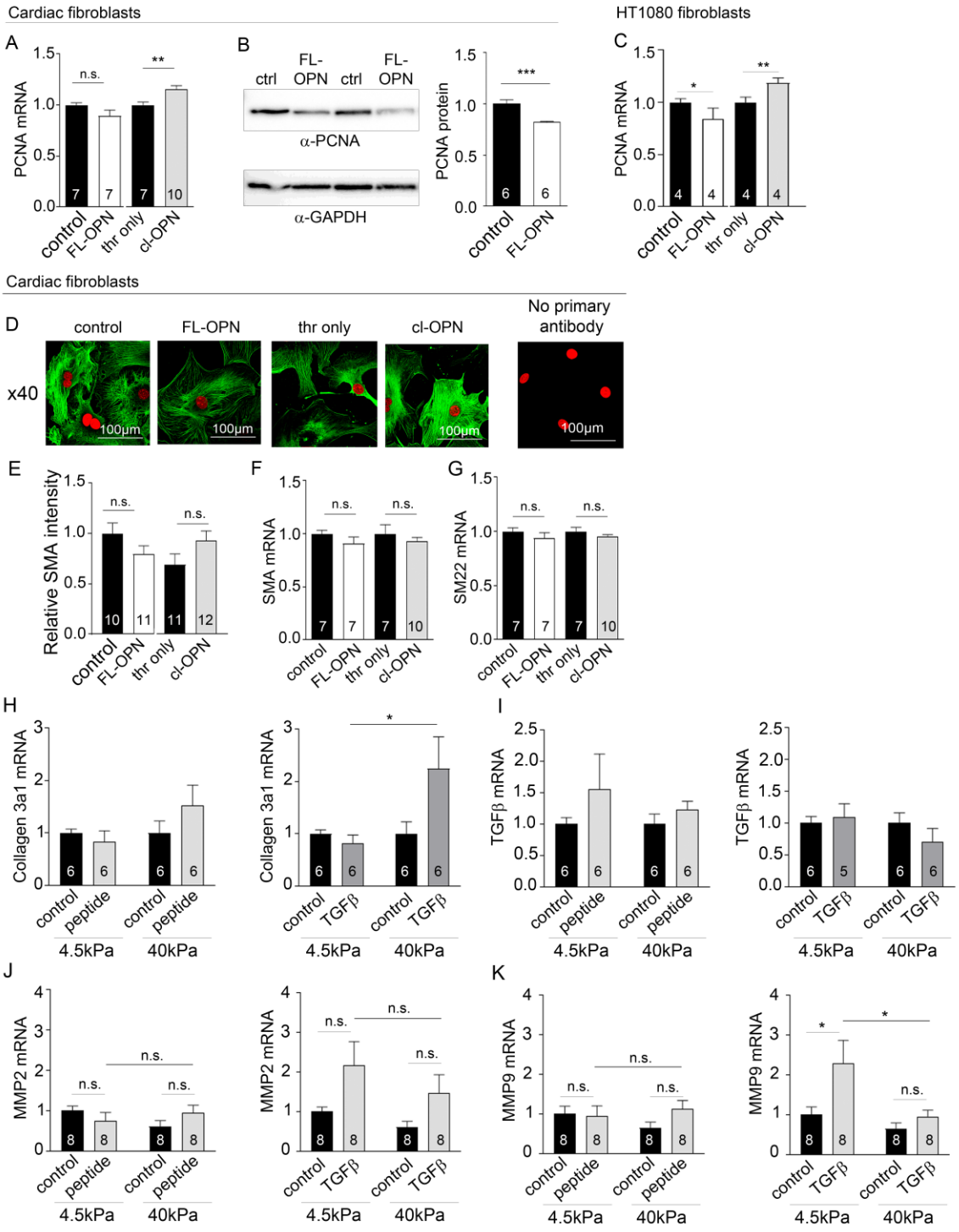

Neonatal cardiac fibroblasts (A,B D-G), adult cardiac fibroblasts (H-K) and HT1080 fibroblasts (C) stimulated with full-length (FL-OPN), thrombin-cleaved OPN (cl-OPN), thrombin, RGDSLAYGLR peptide and TGFβ. Proliferation was determined by expression of proliferating cell nuclear antigen (PCNA; A-C). Myofibroblast differentiation was determined by immunostaining for smooth muscle α-actin (SMA; D and E) and expression of SMA (F) and SM22 (G). Collagen3a1 (H), TGFβ (I), MMP2 (J) and MMP9 (K) mRNA normalized to glyceraldehyde 3-phosphate dehydrogenase (GAPDH). Student's t-test was used in A-G, and two-way ANOVA with Tukey's multiple comparisons test was used in H-K. N are indicated in graphs.

Figure S6. Syndecan-4-osteopontin complex in left ventricular tissue.

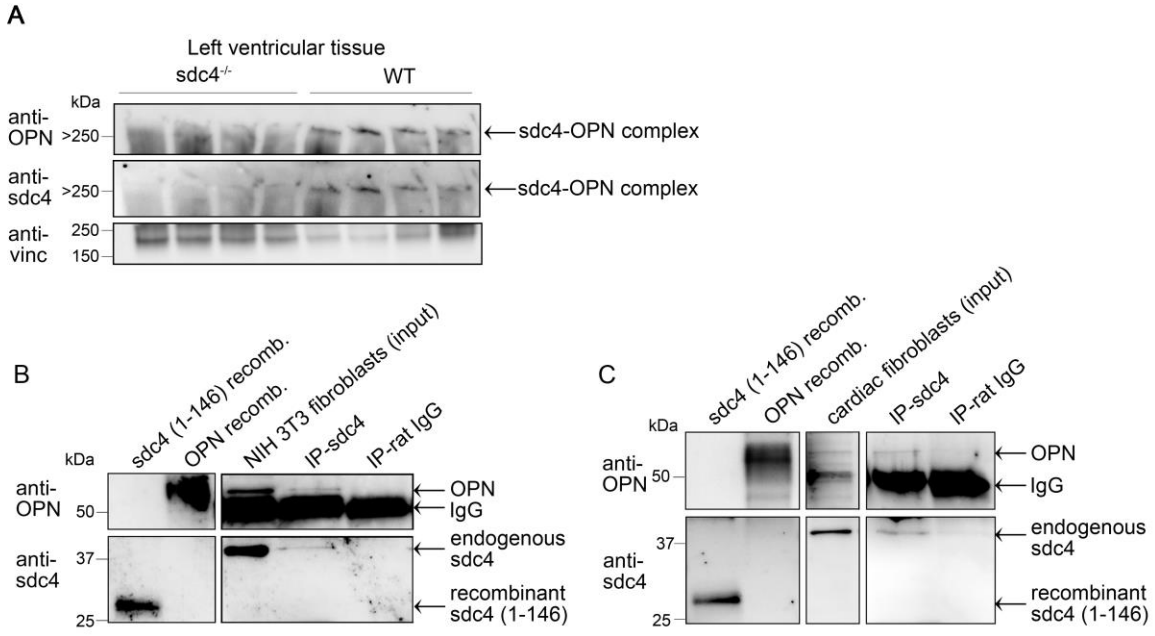

Detection of a syndecan-4 (sdc4)-osteopontin (OPN) high molecular weight complex in left ventricular homogenates from wild-type (WT) mice on native PAGE using antibodies recognizing sdc4 or OPN. Samples are identical to those used in Figure 3A but are here probed with anti-OPN first. Stripping and reprobing with anti-sdc4 confirmed that the two antibodies recognized the same protein complex in WT homogenates. Left ventricle homogenate from sdc4 knockout (sdc4-/-) mice was used as negative control (lane 1-4). Vinculin (vinc) was used as loading control. (B and C) Immunoprecipitation of sdc4-OPN complex in cell lysates from NIH3T3 fibroblasts (B) and primary neonatal cardiac fibroblasts from rat (C). Same blot as in Figure 3B and C but without cropping IgG band.

Figure S7. Ca^{2+} does not prevent cleavage of OPN by thrombin.

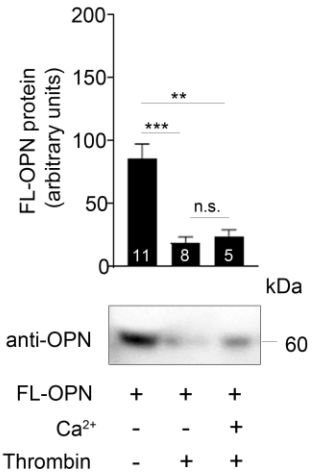

Recombinant full-length osteopontin (FL-OPN) protein levels following incubation with 2 mM Ca2+ and thrombin. One-way ANOVA with Holm-Sidak's multiple comparisons was used to determine significant differences. N are indicated in graphs.

Figure S8. Cytokines of sterile inflammation are rapidly increased in response to pressure overload.

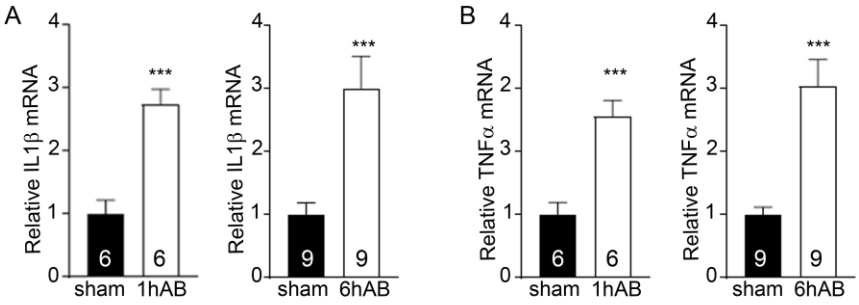

Left ventricular interleukin (IL)-1β (A) and tumor necrosis factor (TNF) α (B) mRNA in sham operated mice and mice subjected 1h and 6h aortic banding (AB). mRNA levels were to normalized to glyceraldehyde 3-phosphate degydrogenase (GAPDH). Student's t-test was used to determine significant differences between AB and sham for each time point. N are indicated in graphs.

Figure S9. Validation of the osteopontin blocking peptide.

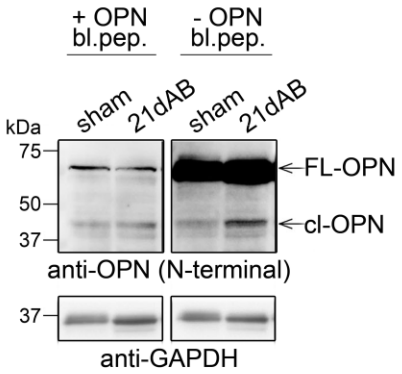

Immunoblot analysis of FL-OPN and cl-OPN after 21 days AB showing samples as in Figure 5C, using anti-OPN (ab181440) primary antibody with and without the custom made osteopontin (OPN) blocking peptide (bl. pep; amino acids 53-84 in mouse OPN: LLAPQNAVSSEEKDDFKQETLPSNSNESHDHM).

Figure S10. In vivo expression of matrix metalloproteinase (MMP) and tissue inhibitor of metalloproteinases (TIMP).

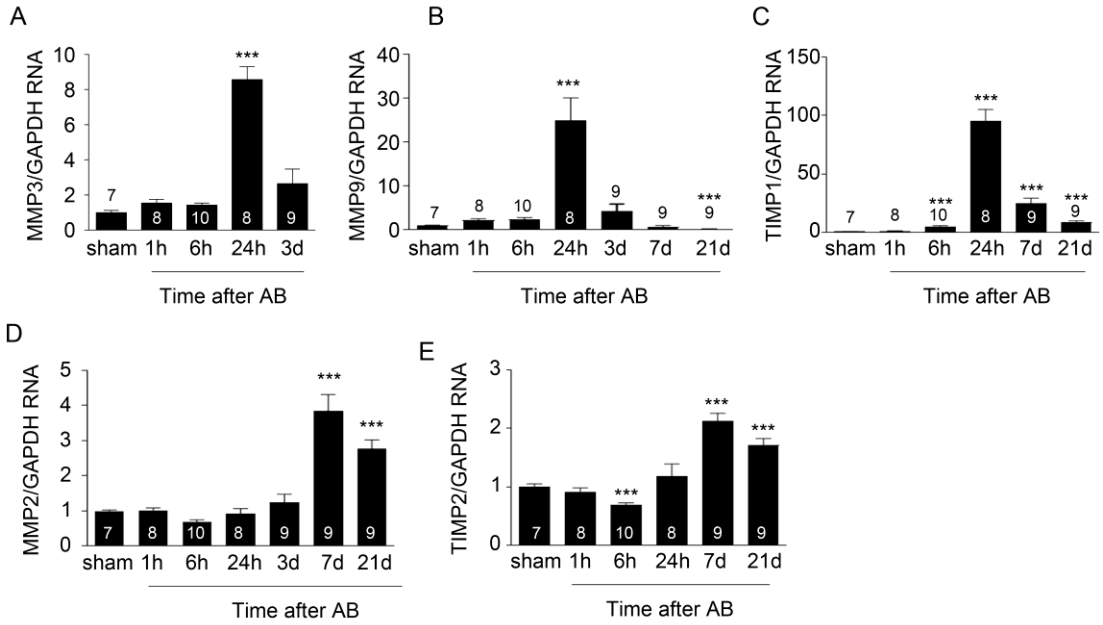

MMP2, MMP3, MMP9, TIMP1 and TIMP2 mRNA normalized to GAPDH mRNA in left ventricular tissue lysates at different time points after aortic banding (AB). The 7 day time point was published in[2]. N are indicated in graphs.

Supplemental References:

1. Braathen B, Tonnessen T. Cold blood cardioplegia reduces the increase in cardiac enzyme levels compared with cold crystalloid cardioplegia in patients undergoing aortic valve replacement for isolated aortic stenosis. *J Thorac Cardiovasc Surg.* 2010;139:874-80.
2. Herum KM, Lunde IG, Skrbic B, Louch WE, Hasic A, Boye S, Unger A, Brorson SH, Sjaastad I, Tønnessen T, Linke WA, Gomez MF, Christensen G. Syndecan-4 is a key determinant of collagen cross-linking and passive myocardial stiffness in the pressure-overloaded heart. *Cardiovasc Res.* 2015;106:217-26.